GEOPHYSICS, VOL. 85, NO. 3 (MAY-JUNE 2020); P. T209–T224, 10 FIGS., 1 TABLE.
10.1190/GEO2019-0665.1

Seismic Q of inhomogeneous plane waves in porous media

Xu Liu[1], Stewart Greenhalgh[1], and José M. Carcione[2]

ABSTRACT

Seismic waves in an attenuative porous medium are generally inhomogeneous waves, which have different directions of propagation and attenuation. The dissipation factors ($1/Q$) of inhomogeneous waves are strongly dependent on the degree of wave inhomogeneity and cannot be expressed correctly with the usual $1/Q$ expressions valid only for homogeneous waves. We have used the differing definitions of $1/Q$ for inhomogeneous waves (i.e., the ratio of the time-averaged dissipated energy density to the time-averaged strain energy density or time-averaged total energy density) and the complex form of the energy balance equations of poroviscoelastic media to derive concise and explicit expressions for the dissipation factors. They are given as simple functions of the material parameters and the wave inhomogeneity parameter for inhomogeneous SV-waves and fast and slow P-waves. The isotropic, poroviscoelastic medium under consideration is upscaled from effective Biot theory for a double-porosity solid, which is the most general theory to describe wave propagation in a reservoir. We find that, if the inhomogeneity parameter is infinite (i.e., the inhomogeneity angle is 90°) for all three Biot waves, then the dissipation factors only depend on the ratio of the imaginary to the real part of the complex shear modulus. Our explicit expressions for the dissipation factors of poroviscoelastic materials also are reduced to obtain their counterparts for viscoelastic media as a special case. The inhomogeneous waves in an example poroviscoelastic material are used to demonstrate that the $1/Q$ values of the three Biot waves strongly depend on the inhomogeneity parameters and furthermore the different definitions may cause significant differences of $1/Q$ values. We find that the dissipation factor of fast P-waves may decrease with the increasing degree of inhomogeneity, which contradicts previously published results.

INTRODUCTION

Most materials near the earth's surface, especially porous reservoirs, are dissipative with significant intrinsic energy absorption. The seismic waves propagating in such materials are generally inhomogeneous waves; that is, they do not have the same propagation and maximum attenuation directions (Lockett, 1962). The degree of wave inhomogeneity can significantly change the phase velocity, attenuation factor, and other properties that are the fundamental characteristics of the waves. Such waves are far from being well-studied, especially for porous reservoirs such as in petroleum exploration, geothermal investigations, and groundwater search. Therefore, it is of critical importance to investigate the dependence of these characteristics on the degree of wave inhomogeneity. The damping or anelastic property of seismic waves commonly is represented by the inverse quality factor Q^{-1} (also called the dissipation factor). The dimensionless quantity Q^{-1} generally is defined as the ratio of the time-averaged dissipated energy density to the time-averaged strain energy density (denoted as Q_V^{-1}; see Carcione, 2014). An alternative definition replaces the denominator in the ratio with the time-averaged energy density (denoted as Q_T^{-1}; see Buchen, 1971). For homogeneous waves in isotropic media, which have the same directions of propagation and attenuation, there are two alternative definitions of the dissipation factor: (1) Q_V^{-1}, which can be expressed as the ratio of the imaginary part of the squared complex wavenumber k over the real part, $Q_V^{-1} = \mathrm{Im}(k^2)/\mathrm{Re}(k^2)$, and (2) Q_T^{-1}, which can be written as the following function of the attenuation coefficient α, phase velocity v, and frequency ω: $Q^{-1} = 2\alpha v/\omega$ (Carcione, 2014). Therefore, these equations actually are viewed as the general definition of Q^{-1} in many publications.

Manuscript received by the Editor 15 October 2019; revised manuscript received 18 January 2020; published ahead of production 16 March 2020; published online 29 April 2020.
[1]King Fahd University of Petroleum and Minerals, College of Petroleum Engineering & Geosciences, PO Box 5086, Dhahran, Saudi Arabia. E-mail: liu.xu@kfupm.edu.sa (corresponding author); greenhalgh@kfupm.edu.sa.
[2]Istituto Nazionale di Oceanografia e di Geofisica Sperimentale (OGS), Borgo Grotta Gigante 42c, 34010 Sgonico, Trieste, Italy. E-mail: jcarcione@inogs.it.

However, for highly dissipative media, inhomogeneous waves (in which the propagation direction is not parallel to the attenuation vector), these different definitions of Q^{-1} can lead to significant differences, which must be clarified. This is especially the case for seismic waves in porous media, where the definition Q_V^{-1} for homogeneous waves can result in negative or even infinite values for Q^{-1}, which obviously is inadmissible.

The most popular theory to describe seismic wave propagation in a porous solid (e.g., a petroleum reservoir) is Biot theory. According to the classic Biot theory (Biot, 1956a, 1956b, 1962a, 1962b), in a homogeneous material the only energy dissipation mechanism is called Biot global flow, which is created at the scale of a wavelength. There is a relative displacement between the solid and the viscous fluid in the pore space, which takes energy out of the wave. Biot theory predicts that there are typically three types of seismic wave in a porous solid, that is, the S-wave and the fast and the slow P-waves; in this paper, they are denoted respectively as the S-, P1-, and P2-wave for simplicity.

The classic Biot theory when applied to homogeneous media (inhomogeneity of the medium should not be confused with inhomogeneity of the wave, which refers to amplitude variations on the wavefront) cannot explain the high level of attenuation in the seismic frequency range (i.e., 1–1000 Hz) observed in actual reservoirs. Based on the double-porosity and dual-permeability (DPDP) model (Pride et. al., 2004), effective Biot theory can explain this high-level attenuation with the inner flow dissipation mechanism. It arises from material inhomogeneity at the mesoscopic scale in which there are two porous phases present having dissimilar compressibilities and permeabilities such that, during the passage of a P-wave, there is local fluid flow between them. Therefore, in effective Biot theory, there are two dissipation mechanisms: inner flow and Biot global flow. However, the DPDP model, to date, has been developed only for P- but not S-waves. Liu et al. (2018) uspscale and generalize effective Biot theory to the poroviscoelastic model, which will be used to investigate the dissipation factors of the three Biot waves (S-, P1-, and P2-waves) in this paper.

Unlike the S- and P1-waves, P2-waves are thought to be diffusive in the low-frequency range and only rarely have been observed experimentally in synthetic water-saturated sandstone (Plona, 1980) and natural water-saturated sandstone (Kelder and Smeulders, 1997). It has been determined that the definition $Q^{-1} = -\mathrm{Im}(M)/\mathrm{Re}(M)$ (where M is the complex modulus) is not suitable for P2-waves because, for diffusive modes, the real part of the complex modulus Re(M) tends to zero (or equally, as stated by Berryman and Wang [2000], the imaginary and real parts of the complex velocity are of comparable size). This means that Q^{-1} could tend to infinity or even negative values. The latter is unacceptable from a physical point of view, but $Q = 0$ holds for a pure diffusion equation in which all energy is dissipated and none is stored.

To avoid the above complication, Berryman and Wang (2000) use the definition $Q^{-1} = 2\alpha v/\omega$ in all cases, by which the Q^{-1} of the P2-waves is calculated to be close to 2 (for low frequency). Possibly for the same reason, this definition also is used in other publications for Biot waves, for example, Badiey et al. (1998), Chen (2016), and Turgut and Yamamoto (1988). However, it must be understood that the definition $Q^{-1} = 2\alpha v/\omega$ is under the assumption of homogeneous waves, which will not be correct for inhomogeneous waves.

Because of the high-level attenuation observed in near-surface formations and petroleum reservoirs, seismic waves are generally inhomogeneous. The P2-waves are much more highly attenuative than P1- or S-waves. Therefore, it is very important to investigate the dissipation factors of waves in a reservoir directly from the definitions Q_V^{-1} and Q_T^{-1} with proper consideration of the inhomogeneity of the wave.

The dissipation features of inhomogeneous viscoelastic waves have been investigated over many decades (e.g., Buchen, 1971; Borcherdt, 1977, 1982, 2009; Borcherdt and Wennerberg, 1985; Carcione and Cavallini, 1993; Cerveny and Psencik, 2005, 2006). We have found that explicit formulas for Q^{-1} have been provided first by Borcherdt and Wennerberg (1985) for viscoelastic materials (not for porous media). Here, the word "explicit" is taken to mean that the Q^{-1} formulas are expressed as functions of the known material parameters and the degree of wave inhomogeneity, that is, the inhomogeneity parameter D or the inhomogeneity angle γ (Buchen, 1971; Cerveny and Psencik, 2005). Their Q^{-1} formulas are under the definition as the ratio of the time-averaged dissipated energy density to the peak potential (strain) energy density normalized by 2π (denoted as Q_B^{-1}; see Borcherdt, 1977). However, different definitions of Q^{-1} may result in different values of Q^{-1} for dissipative and inhomogeneous waves. Therefore, Q_B^{-1} may be very different from Q_V^{-1} and Q_T^{-1}, even for viscoelastic materials (Liu et al., 2020). Liu et al. (2020) present explicit Q^{-1} formulas of viscoelastic materials under the definitions of Q_V^{-1} and Q_T^{-1}. Considering the relative movement between the pore fluid and the porous solid frame, the poroviscoelastic model has much more complicated wave equations than those of the viscoelastic model because the extra equations to describe the fluid movement are integrated into the wave equations (Biot, 1956a, 1956b, 1962a, 1962b; Pride et al., 2004; Liu et al., 2018). Therefore, the viscoelastic model is the special case of the poroviscoelastic model when the relative movement of the pore fluid is ignored. However, various mechanisms of the relative movement of the pore fluid are of critical importance for describing seismic wave attenuation in near-surface formations and petroleum reservoirs. It is obviously very important to investigate the dissipation factors based on the poroviscoelastic model. To the best of our knowledge, no explicit formulas have been published for porous media under the definitions of Q_V^{-1} and Q_T^{-1}.

In the following sections, we derive explicit, novel formulas for the dissipation factors Q^{-1} under the definitions of Q_V^{-1} and Q_T^{-1} for the three Biot waves in effective Biot materials, thus unifying and generalizing the treatment for the first time. Then, these results for poroviscoelastic materials are reduced to obtain their counterpart equations for viscoelastic media as a special case. With an example effective Biot material, we show how to use these explicit formulas and investigate how the inhomogeneity degree of a plane wave affects the dispersion characteristics of such waves propagating in poroviscoelastic media. Because our equations are derived in the x-z coordinate plane, the S-waves in our paper refer to the SV-waves.

EFFECTIVE BIOT THEORY AND THE UPSCALED POROVISCOELASTIC MODEL

In the frequency domain, the classic Biot wave equations (Biot, 1962a, 1962b) and the effective Biot equations (Pride et al., 2004) have a very similar form. But the effective Biot equations are more general than the classic Biot equations in that the Biot elastic coefficients all become frequency dependent and can be well-approximated with the general fractional Zener model (upscaled

poroviscoelastic model; see Liu et al., 2018). If these coefficients are set as frequency independent, the effective Biot theory reduces to the classic Biot theory. Therefore, our investigation is based on the effective Biot equations whose wave equations (source terms ignored) can be written as

$$\begin{aligned}&[(H-G)\nabla\nabla+(G\nabla^2+\omega^2\rho)\mathbf{I}]\cdot\mathbf{u}+[C\nabla\nabla+\omega^2\rho_f\mathbf{I}]\cdot\mathbf{w}=0\\&[C\nabla\nabla+\omega^2\rho_f\mathbf{I}]\cdot\mathbf{u}+[M\nabla\nabla+\omega^2\tilde{\rho}(\omega)\mathbf{I}]\cdot\mathbf{w}=0,\end{aligned}\tag{1}$$

where $\mathbf{u}$ is the solid particle displacement and $\mathbf{w}=\varphi(\mathbf{U}-\mathbf{u})$ is the relative fluid displacement multiplied by material porosity φ. Here, $\mathbf{U}$ represents the absolute fluid displacement in an inertial reference frame. For density terms ρ and $\tilde{\rho}(\omega)$ in equation 1, $\rho=\varphi\rho_f+(1-\varphi)\rho_g$, $\tilde{\rho}(\omega)=i\eta/[\omega k^*(\omega)]$ and ρ_g is the grain density; ρ_f and η are the density and viscosity of the fluid, and $k^*(\omega)$ is the effective dynamic permeability (Liu et al., 2018).

The elastic coefficients M, C, and H can be written as functions of the frequency-dependent shear and bulk moduli of the solid frame, that is, $G(\omega)$ and $K^d(\omega)$ (for details, see Pride et. al., 2004); together with constant grain bulk modulus K^g and fluid bulk modulus K^f,

$$\begin{cases}\frac{1}{M}=\frac{\alpha}{K^g}+\phi\left(\frac{1}{K^f}-\frac{1}{K^g}\right), & \alpha=1-\frac{K^d}{K^g}\\ H=K^d+4G/3+\alpha^2M, & C=\alpha M\end{cases}.\tag{2}$$

Because G and K^d are frequency dependent, it follows that M, C, and H are also functions of frequency.

Liu et al. (2018) suggest a method based on the general fractional Zener model to upscale effective Biot theory to a poroviscoelastic model covering P- and S-waves and in which a complex modulus $Z(\omega)$ (representing $G(\omega)$ and $K^d(\omega)$) can be written as $Z(\omega)=Z(\omega=0)\Omega_Z(\omega)$ with

$$\Omega_Z(\omega)=\frac{1}{L_Z}\sum_{l=1}^{L_Z}[1+(-i\omega\tau_{\varepsilon l}^Z)^{\alpha l}]/[1+(-i\omega\tau_{\sigma l}^Z)^{\alpha l}].\tag{3}$$

In this equation, $\Omega_Z(\omega)$ is the relaxation function, $Z(\omega=0)$ is the relaxed modulus that is assumed to be known, L_Z is the number of model elements used, $\tau_{\sigma l}^Z$ and $\tau_{\varepsilon l}^Z$ are the stress and strain relaxation times, respectively, and αl is the fractional derivative order. If $L_Z=1$, the equation reverts to the famous Cole-Cole model (e.g., Picotti and Carcione, 2017). If $\Omega_Z(\omega)=1$, we obtain the result of the classic Biot model.

INHOMOGENEOUS PLANE WAVES AND THE CHRISTOFFEL EQUATION OF EFFECTIVE BIOT MEDIA

For inhomogenous plane waves in poroviscoelastic media, the time-averaged stored and dissipated energy densities (Carcione and Cavallini, 1993; Carcione, 2014) are expressed as the product of the extended wavefield vectors and the elasticity (and/or generalized mass density) matrix. Although the cited formulas are obtained based on classic Biot theory, they are in a form similar to the equations of effective Biot theory in the frequency domain, as stated previously. To apply these equations for caluclating the dissipation factors of the three Biot waves, we need to decompose the effective Biot wave equations without the assumption of a homogeneous wave and determine the eigencharacteristics that include the frequency dependence of the complex wave velocities and the coefficients specifying the ratio between the solid and relative fluid displacements to construct the extended inhomogeneous plane wave field vectors.

The solid particle displacement $\mathbf{u}$ and the fluid displacement relative to the solid $\mathbf{w}$ of inhomogeneous plane waves in an effective Biot material can be written as

$$\begin{aligned}\mathbf{u}(\mathbf{r},t)&=\tilde{\mathbf{u}}\exp[i\omega(\mathbf{p}\cdot\mathbf{r}-t)]\\ \text{and}\quad \mathbf{w}(\mathbf{r},t)&=\tilde{\mathbf{w}}\exp[i\omega(\mathbf{p}\cdot\mathbf{r}-t)],\end{aligned}\tag{4}$$

where $\tilde{\mathbf{u}}$ and $\tilde{\mathbf{w}}$ are the complex vector amplitudes and $\mathbf{p}$ is the complex slowness vector. Following Cerveny and Psencik (2005, 2006), the complex slowness is written as

$$\mathbf{p}=\sigma\hat{\mathbf{n}}+iD\hat{\mathbf{m}}\quad\text{or}\quad\mathbf{p}=p\hat{\mathbf{p}},\tag{5}$$

where σ is the complex slowness. The real-valued unit vector $\hat{\mathbf{n}}$ is called the propagation direction; the real-valued tangent unit vector $\hat{\mathbf{m}}$ is perpendicular to $\hat{\mathbf{n}}$ (or $\hat{\mathbf{m}}\cdot\hat{\mathbf{n}}=0$) and represents the attenuation direction (defining the complex dual wave vector $\mathbf{p}$). The real-valued quantity D refers to the inhomogeneity parameter and relates to the inhomogeneity angle γ between the propagation direction and the maximum attenuation direction through $\cos(\gamma)=\mathrm{Im}(\sigma)/\sqrt{\mathrm{Im}^2(\sigma)+D^2}$. The terms D and γ represent the degree of inhomogeneity of the wave. The ranges of these inhomogeneity parameters are $-\infty\le D\le\infty$ and $-\pi/2\le\gamma\le\pi/2$. Quantity p represents the complex slowness that depends on the material parameters and will be solved from the following Christoffel equation. The unit vector $\hat{\mathbf{p}}$ is complex ($\hat{\mathbf{p}}\cdot\hat{\mathbf{p}}=1$).

Using equation 5, we have

$$\mathbf{p}\cdot\mathbf{p}=p^2=(\sigma\hat{\mathbf{n}}+iD\hat{\mathbf{m}})\cdot(\sigma\hat{\mathbf{n}}+iD\hat{\mathbf{m}})=\sigma^2-D^2.\tag{6}$$

With equation 6, we have

$$p^2=\sigma^2-D^2\quad\text{or}\quad\sigma^2=p^2+D^2.\tag{7}$$

For a given material, the p does not change with D, but the complex σ will change with D.

The phase velocity is defined as

$$v^{pv}=1/\mathrm{Re}(\sigma),\tag{8}$$

where the symbols $\mathrm{Re}(\bullet)$ and $\mathrm{Im}(\bullet)$ represent the real and imaginary parts of a quantity. Substituting $\sigma=\mathrm{Re}(\sigma)+i\,\mathrm{Im}(\sigma)$ and $p=\mathrm{Re}(p)+i\,\mathrm{Im}(p)$ into equation 7, the real and the imaginary parts become

$$\left.\begin{aligned}\mathrm{Re}^2(\sigma)=&0.5\left[\mathrm{Re}^2(p)-\mathrm{Im}^2(p)+D^2\right.\\&\left.+\sqrt{[\mathrm{Re}^2(p)-\mathrm{Im}^2(p)+D^2]^2+4\mathrm{Re}^2(p)\mathrm{Im}^2(p)}\right]\\ \mathrm{Im}(\sigma)=&\mathrm{Re}(p)\mathrm{Im}(p)/\mathrm{Re}(\sigma)\end{aligned}\right\}. \quad (9)$$

Equation 9 implies that increasing the absolute value of D, hereafter denoted as $|D|$, results in increasing slowness $\mathrm{Re}(\sigma)$ and thus decreasing phase velocity according to equation 8. Increasing $|D|$ or increasing slowness $\mathrm{Re}(\sigma)$ will cause a decrease in $\mathrm{Im}(\sigma)$, but it is uncertain whether this will cause a decrease in the dissipation factor Q^{-1} for inhomogeneous waves. The Q^{-1} needs to be calculated according to different definitions.

In a manner similar to the treatment of electroseismic waves by Pride and Haartsen (1996), substituting equation 4 into equation 1 produces

$$\begin{bmatrix}\mathbf{A} & \mathbf{B}\\ \mathbf{E} & \mathbf{D}\end{bmatrix}\begin{bmatrix}\tilde{\mathbf{w}}\\ \tilde{\mathbf{u}}\end{bmatrix}=\begin{bmatrix}0\\0\end{bmatrix}, \quad (10)$$

where

$$\begin{bmatrix}\mathbf{A} & \mathbf{B}\\ \mathbf{E} & \mathbf{D}\end{bmatrix}=\begin{bmatrix}\tilde{\rho}\mathbf{I}-M\mathbf{pp} & \rho_f\mathbf{I}-C\mathbf{pp}\\ \rho_f\mathbf{I}-C\mathbf{pp} & (\rho-Gp^2)\mathbf{I}-(H-G)\mathbf{pp}\end{bmatrix}, \quad (11)$$

and $\mathbf{I}$ is the identity matrix or tensor. The tensor $\mathbf{pp}$ can be viewed as the dyadic product $\mathbf{pp}^T$ where $\mathbf{p}^T$ denotes the transpose of $\mathbf{p}$. Equation 10 also can be written as

$$\tilde{\mathbf{w}}=-\mathbf{A}^{-1}\mathbf{B}\tilde{\mathbf{u}} \text{ or } \tilde{\mathbf{w}}=-\mathbf{E}^{-1}\mathbf{D}\tilde{\mathbf{u}}. \quad (12)$$

The Christoffel equation takes the form

$$[\mathbf{A}^{-1}\mathbf{B}-\mathbf{E}^{-1}\mathbf{D}][\tilde{\mathbf{u}}]=[R_S\mathbf{I}+R_Pp^2\hat{\mathbf{p}}\,\hat{\mathbf{p}}][\tilde{\mathbf{u}}]=[0], \quad (13)$$

where

$$R_S=\rho_f/\tilde{\rho}-(\rho-Gp^2)/\rho_f, \quad (14)$$

$$R_P=\frac{(H-G)}{\rho_f}-\frac{C}{\tilde{\rho}}+\frac{(\rho-Gp^2)-(H-G)p^2}{\rho_f(p^2-\rho_f/C)}+\frac{Cp^2-\rho_f}{\tilde{\rho}(p^2-\tilde{\rho}/M)}. \quad (15)$$

The secular determinant of equation 13 has three complex roots (eigenvalues) with corresponding eigenvectors or complex vector amplitudes (Pride and Haartsen, 1996). The root of p^2 given by $R_S=0$ corresponds to the S-wave slowness $p^{(1)}$ with its eigenvector, or complex amplitude vector $\tilde{\mathbf{u}}_T$ given as

$$p^{(1)}=\sqrt{(\rho-\rho_f^2/\tilde{\rho})/G}, \quad \tilde{\mathbf{u}}_T\cdot\hat{\mathbf{p}}^{(1)}=0. \quad (16)$$

Combining equations 11, 12, and 16 produces

$$\tilde{\mathbf{w}}_T=\xi^{(1)}\tilde{\mathbf{u}}_T, \quad \xi^{(1)}=-\rho_f/\tilde{\rho}=G(p^2-\rho/G)/\rho_f. \quad (17)$$

The complex coefficients $\xi^{(k)}$ specify the ratio between the solid and the relative fluid displacements.

Similarly, the other roots of p^2 for $R_S+R_Pp^2=0$ correspond to two longitudinal waves: the P1- and P2-waves, respectively, having slownesses $p^{(2)}$ and $p^{(3)}$, respectively, and their eigenvectors $\tilde{\mathbf{u}}_L$ given by

$$\left.\begin{aligned}(p^{(2,3)})^2=&\tfrac{1}{2}\left[b\pm\sqrt{b^2-4(\rho\tilde{\rho}-\rho_f^2)/(HM-C^2)}\right]\\ b=&(H\tilde{\rho}-2C\rho_f+M\rho)/(HM-C^2)\end{aligned}\right\},\ \tilde{\mathbf{u}}_L=c\hat{\mathbf{p}}. \quad (18)$$

Here, c is an arbitrary scalar. In a manner similar to equation 17, we obtain

$$\tilde{\mathbf{w}}_L=\xi^{(k)}\tilde{\mathbf{u}}_L,\ \xi^{(k)}=\frac{\rho_f-C(p^{(k)})^2}{(p^{(k)})^2M-\tilde{\rho}}=-\frac{H(p^{(k)})^2-\rho}{C(p^{(k)})^2-\rho_f}\ (k=2,3). \quad (19)$$

THE COMPLEX FORM OF THE ENERGY BALANCE EQUATION

The complex form of the energy balance equation of a poroviscoelastic material is given by Carcione (2014) as follows. Note, because the time dependence of harmonic waves in our paper is assumed to be $\exp(-i\omega t)$, whereas Carcione uses a positive exponential, the negative sign involving with the time derivative has been adjusted accordingly. The formula is

$$\begin{aligned}-\mathrm{div}\left(\sum\cdot\mathbf{v}^*\right)=&2i\omega\left[\frac{1}{4}\mathrm{Re}(\mathbf{v}^*\cdot\mathbf{R}\cdot\mathbf{v})-\frac{1}{4}\mathrm{Re}(\mathbf{e}^T\cdot\mathbf{P}\cdot\mathbf{e}^*)\right]\\&+2\omega\left[-\frac{1}{4}\mathrm{Im}(\mathbf{v}^*\cdot\mathbf{R}\cdot\mathbf{v})+\frac{1}{4}\mathrm{Im}(\mathbf{e}^T\cdot\mathbf{P}\cdot\mathbf{e}^*)\right].\end{aligned} \quad (20)$$

Here, $\mathbf{v}$ is the extended particle velocity vector

$$\mathbf{v}=(\dot{u}_1,\dot{u}_2,\dot{u}_3,\dot{w}_1,\dot{w}_2,\dot{w}_3)^T, \quad (21)$$

$\sum$ is the extended stress tensor, $\mathbf{P}$ is the elasticity matrix, and $\mathbf{R}$ is the mass density matrix. The extended strain array $\mathbf{e}$ can be expressed with the solid displacement $\mathbf{u}$ and the relative fluid displacement $\mathbf{w}$:

$$\mathbf{e}=(e_1,e_2,e_3,e_4,e_5,e_6,-\zeta)^T, \quad (22)$$

where

$$\begin{aligned}&e_1=\partial_1u_1, \quad e_2=\partial_2u_2, \quad e_3=\partial_3u_3, \quad e_4=\partial_2u_3+\partial_3u_2,\\&e_5=\partial_1u_3+\partial_3u_1, \quad e_6=\partial_1u_2+\partial_2u_1;\end{aligned} \quad (23)$$

and

$$\zeta=-div\mathbf{w}, \quad \mathbf{w}=\varphi(\mathbf{U}-\mathbf{u}). \quad (24)$$

This complex energy balance equation has been developed for porous and anisotropic media (Carcione, 2014). But, here we only consider isotropic porous media. For the sake of completeness, $\sum$ and the isotropic versions of $\mathbf{P}$ and $\mathbf{R}$ are provided in Appendix A. In equation 20, the vector $-\sum \cdot \mathbf{v}^*/2$ is the Umov-Poynting vector that describes the energy flux. The physical meanings of the other terms are described as follows.

The time-averaged strain energy density $\langle V \rangle$ is given by

$$\langle V \rangle = \frac{1}{4}\mathrm{Re}(\mathbf{e}^{\mathbf{T}} \cdot \mathbf{P} \cdot \mathbf{e}^*) = \frac{1}{4}\mathrm{Re}(V^c). \tag{25}$$

Here, we call $\mathbf{e}^{\mathbf{T}} \cdot \mathbf{P} \cdot \mathbf{e}^*$ the complex strain energy density, denoted as V^c given by equation A-4 in Appendix A.

The time-averaged kinetic energy density $\langle T \rangle$ is written with the extended particle velocity array $\mathbf{v}$ and the generalized mass density matrix $\mathbf{R}$:

$$\langle T \rangle = \frac{1}{4}\mathrm{Re}(\mathbf{v}^{*T} \cdot \mathbf{R} \cdot \mathbf{v}) = \frac{1}{4}\mathrm{Re}(T^c). \tag{26}$$

Here, we call $\mathbf{v}^{(*)T} \cdot \mathbf{R}^{(*)} \cdot \mathbf{v}$ the complex kinetic energy density, denoted as T^c given by equation A-5 in Appendix A. The term $\mathbf{v}$ is given by equation 21.

The time-averaged strain dissipated energy density $\langle D_V \rangle$ and the kinetic dissipated energy density $\langle D_T \rangle$ are given by Carcione (2014) as

$$\langle D_V \rangle = -\frac{1}{2}\mathrm{Im}(V^c) = -\frac{1}{2}\mathrm{Im}(\mathbf{e}^T \cdot \mathbf{P} \cdot \mathbf{e}^*), \tag{27}$$

$$\langle D_T \rangle = \frac{1}{2}\mathrm{Im}(T^c) = \frac{1}{2}\mathrm{Im}(\mathbf{v}^{(*)T} \cdot \mathbf{R} \cdot \mathbf{v}). \tag{28}$$

EXPLICIT DISSIPATION FACTORS FOR INHOMOGENEOUS WAVES IN EFFECTIVE BIOT MATERIALS

For a given wave type k ($k = 1,2,3$ for S-, P1-, and P2-waves, respectively), the solid particle displacement $\mathbf{u}^{(k)}$ and the relative fluid displacement $\mathbf{w}^{(k)}$ can be written as

$$\mathbf{u}^{(k)} = \tilde{\mathbf{u}}^{(k)} \exp[i\omega(\mathbf{p}^{(k)} \cdot \mathbf{r} - t)], \quad \mathbf{w}^{(k)} = \xi^{(k)}\mathbf{u}^{(k)}. \tag{29}$$

Here, $\tilde{\mathbf{u}}^{(k)}$ is the complex vector amplitude of wave type k. The coefficients $\xi^{(k)}$ are specified in equations 17 and 19. For the sake of simplicity, we will remove the superscript (k) without causing confusion. Furthermore, without loss of generality, we consider only the 2D case. For an inhomogeneous wave propagating in the x-z plane along the z-direction, the propagation direction is written as $\hat{\mathbf{n}} = (0,0,1)$ with its orthogonal direction in the x-z plane as $\hat{\mathbf{m}} = (1,0,0)$. Using equation 5, the complex slowness along direction $\hat{\mathbf{n}}$ is calculated as σ. Thus, the slowness vector $\mathbf{p}$ is written as $(p_x, 0, p_z)$

$$\mathbf{p} = (p_x, 0, p_z) = \sigma\hat{\mathbf{n}} + iD\hat{\mathbf{m}} = \sigma(0,0,1) + iD(1,0,0) \tag{30}$$

or

$$p_x = iD, \quad p_z = \sigma. \tag{31}$$

After the complex slowness vector $\mathbf{p}$ is determined, the complex amplitudes are defined according to the eigenvectors of the corresponding wave types (equations 16 and 18).

The solid particle displacement of waves can be written for the S-wave as

$$\mathbf{u} = A(p_z, 0, -p_x)\exp[i\omega(\mathbf{p} \cdot \mathbf{r} - t)] \tag{32}$$

and for the P1- or P2-waves as

$$\mathbf{u} = A(p_x, 0, p_z)\exp[i\omega(\mathbf{p} \cdot \mathbf{r} - t)]. \tag{33}$$

As mentioned in the "Introduction" section, the two most commonly defined dissipation factors are Q_V^{-1} (e.g., Carcione, 2014) and Q_T^{-1} (e.g., Buchen, 1971), which using equations 25, 26, 27, and 28 can be written as

$$Q_V^{-1} = \frac{\langle D_T \rangle + \langle D_V \rangle}{2\langle V \rangle} = \frac{\mathrm{Im}(T^c) - \mathrm{Im}(V^c)}{\mathrm{Re}(V^c)}, \tag{34}$$

$$Q_T^{-1} = \frac{\langle D_T \rangle + \langle D_V \rangle}{\langle T \rangle + \langle V \rangle} = \frac{2\,\mathrm{Im}(T^c) - 2\,\mathrm{Im}(V^c)}{\mathrm{Re}(T^c) + \mathrm{Re}(V^c)}. \tag{35}$$

Comparing equation 34 with 35 indicates that the difference between Q_V^{-1} and Q_T^{-1} depends on the difference between $\langle V \rangle$ and $\langle T \rangle$. If the difference tends to zero, then Q_V^{-1} tends to equal Q_T^{-1}.

The complex strain and kinetic energy densities V^c and T^c of the S-, P1-, and P2-waves, denoted as $V^c_{1,2,3}$ and $T^c_{1,2,3}$, are derived in Appendices B and C for S- and P-waves, respectively. Then, the dissipation factors are obtained for each of the three Biot waves under the definitions of Q_V^{-1} and Q_T^{-1}.

Substituting V_1^c (equation B-5) and T_1^c (equation B-8) into equations 34 and 35 produces the explicit form of the dissipation factors of inhomogeneous S-waves Q_{SV}^{-1} and Q_{ST}^{-1} under the definitions Q_V^{-1} and Q_T^{-1}, respectively:

$$Q_{\mathrm{SV}}^{-1} = \frac{|\xi|^2\mathrm{Im}(\tilde{\rho})(|p^2+D^2|+D^2) - (4D^2|p^2+D^2|+|p^2+2D^2|^2)\mathrm{Im}(G)}{(4D^2|p^2+D^2|+|p^2+2D^2|^2)\mathrm{Re}(G)}. \tag{36}$$

The Q_{SV}^{-1} of a homogeneous wave, that is, $Q_{\mathrm{SV}H}^{-1}$ is obtained as

$$Q_{\mathrm{SV}H}^{-1} = Q_{\mathrm{SV}}^{-1}(D=0) = \frac{|\xi|^2\mathrm{Im}(\tilde{\rho}) - |\sigma_H^2|\mathrm{Im}(G)}{|p^2|\mathrm{Re}(G)}. \tag{37}$$

Liu et al. (2020) mathematically define the dissipation factors at the infinite degree of wave inhomogeneity as the limiting dissipation factors $Q^{-1}(D=\infty)$. The limiting dissipation factor of the

SV-waves under the definition of Q_V^{-1} is obtained by setting $D = \infty$ in equation 36:

$$Q_{\mathrm{SV}}^{-1}(D=\infty) = -\mathrm{Im}(G)/\mathrm{Re}(G). \tag{38}$$

The Q_{ST}^{-1} is given as

$$\left.\begin{aligned} Q_{ST}^{-1} &= \frac{2|\xi|^2\mathrm{Im}(\tilde{\rho})(|p^2+D^2|+D^2) - 2(4D^2|p^2+D^2|+|p^2+2D^2|^2)\mathrm{Im}(G)}{IQD} \\ IQD &= [\rho+\rho_f 2\mathrm{Re}(\xi)+|\xi|^2\mathrm{Re}(\tilde{\rho})](|p^2+D^2|+D^2) \\ &\quad +(4D^2|p^2+D^2|+|p^2+2D^2|^2)\mathrm{Re}(G) \end{aligned}\right\}, \tag{39}$$

The Q_{ST}^{-1} of a homogeneous wave, that is, Q_{STH}^{-1} is obtained as

$$\begin{aligned} Q_{STH}^{-1} &= Q_{ST}^{-1}(D=0) \\ &= 2\frac{|\xi|^2\mathrm{Im}(\tilde{\rho}) - (|p^2|)\mathrm{Im}(G)}{\rho+\rho_f 2\mathrm{Re}(\xi)+|\xi|^2\mathrm{Re}(\tilde{\rho})+(|p^2|)\mathrm{Re}(G)}. \end{aligned} \tag{40}$$

In a manner similar to equation 38, we have the limiting dissipation factor of the SV-waves under the definition of Q_T^{-1}:

$$Q_{ST}^{-1}(D=\infty) = -2\mathrm{Im}(G)/\mathrm{Re}(G). \tag{41}$$

Substituting $V_{2,3}^c$ (equation C-5) and $T_{2,3}^c$ (equation C-7) into equations 34 and 35 produces the explicit form of the dissipation factors for P1-waves $Q_{\mathrm{P1}V}^{-1}$ and P2-waves $Q_{\mathrm{P2}V}^{-1}$ under the definitions Q_V^{-1}; and P1-waves $Q_{\mathrm{P1}T}^{-1}$ and P2-waves $Q_{\mathrm{P2}T}^{-1}$ under the definitions Q_T^{-1}:

$$Q_{\mathrm{P1}V,\mathrm{P2}V}^{-1} = \frac{(|p^2+D^2|+D^2)|\xi|^2\mathrm{Im}\tilde{\rho} - VI_{\mathrm{P1,P2}}}{VR_{\mathrm{P1,P2}}}, \tag{42}$$

where

$$\begin{aligned} VI_{\mathrm{P1,P2}} &= 4D^2|p^2+D^2|\mathrm{Im}(G) + [D^4+|p^2+D^2|^2]\mathrm{Im}(H) \\ &\quad -2D^2[\mathrm{Re}(p^2)+D^2]\mathrm{Im}(\lambda) + 2\mathrm{Re}(\xi)|p^2|^2\mathrm{Im}(C) + |\xi p^2|^2\mathrm{Im}(M), \end{aligned} \tag{43}$$

$$\begin{aligned} VR_{\mathrm{P1,P2}} &= 4D^2|p^2+D^2|\mathrm{Re}(G) + [D^4+|p^2+D^2|^2]\mathrm{Re}(H) \\ &\quad -2D^2[\mathrm{Re}(p^2)+D^2]\mathrm{Re}(\lambda) + 2\mathrm{Re}(\xi)|p^2|^2\mathrm{Re}(C) + |\xi p^2|^2\mathrm{Re}(M). \end{aligned} \tag{44}$$

Note that the subscripts P1, P2 mean that (p, ξ) should be replaced with $(p^{(2)}, \xi^{(2)})$ and $(p^{(3)}, \xi^{(3)})$, respectively.

The $Q_{\mathrm{P1}V,\mathrm{P2}V}^{-1}$ of a homogeneous wave, that is, $Q_{\mathrm{P1}VH,\mathrm{P2}VH}^{-1}$, is obtained as

$$\begin{aligned} Q_{\mathrm{P1}VH,\mathrm{P2}VH}^{-1} &= Q_{\mathrm{P1}V,\mathrm{P2}V}^{-1}(D=0) \\ &= \frac{|\xi|^2\mathrm{Im}\tilde{\rho} - |p^2|[\mathrm{Im}(H)+2\mathrm{Re}(\xi)\mathrm{Im}(C)+|\xi|^2\mathrm{Im}(M)]}{|p^2|[\mathrm{Re}(H)+2\mathrm{Re}(\xi)\mathrm{Re}(C)+|\xi|^2\mathrm{Re}(M)]}. \end{aligned} \tag{45}$$

In a manner similar to equation 38, the limiting dissipation factors of the P1- and P2-waves under the definition of Q_V^{-1} are given as

$$Q_{\mathrm{P1}V,\mathrm{P2}V}^{-1}(D=\infty) = -\mathrm{Im}(G)/\mathrm{Re}(G). \tag{46}$$

The $Q_{\mathrm{P1}T}^{-1}$ and $Q_{\mathrm{P2}T}^{-1}$ are given as

$$Q_{\mathrm{P1}T,\mathrm{P2}T}^{-1} = 2\frac{(|p^2+D^2|+D^2)|\xi|^2\mathrm{Im}(\tilde{\rho}) - VI_{\mathrm{P1,P2}}}{(|p^2+D^2|+D^2)[\rho+2\rho_f\mathrm{Re}(\xi)+|\xi|^2\mathrm{Re}(\tilde{\rho})]+VR_{\mathrm{P1,P2}}}. \tag{47}$$

The $Q_{\mathrm{P1}T,\mathrm{P2}T}^{-1}$ of homogeneous waves, that is, $Q_{\mathrm{P1}TH,\mathrm{P2}TH}^{-1}$, are obtained as

$$\begin{aligned} &Q_{\mathrm{P1}TH,\mathrm{P2}TH}^{-1} \\ &= 2\frac{|\xi|^2\mathrm{Im}\tilde{\rho} - |p^2|[\mathrm{Im}(H)+2\mathrm{Re}(\xi)\mathrm{Im}(C)+|\xi|^2\mathrm{Im}(M)]}{[\rho+2\rho_f\mathrm{Re}(\xi)+|\xi|^2\mathrm{Re}(\tilde{\rho})]+|p^2|[\mathrm{Re}(H)+2\mathrm{Re}(\xi)\mathrm{Re}(C)+|\xi|^2\mathrm{Re}(M)]}. \end{aligned} \tag{48}$$

In a manner similar to equation 41, the limiting dissipation factors of the P1- and P2-waves under the definition of Q_T^{-1} are given as

$$Q_{\mathrm{P1}T,\mathrm{P2}T}^{-1}(D=\infty) = -2\,\mathrm{Im}(G)/\mathrm{Re}(G). \tag{49}$$

Note that, for the P1-waves, p will be replaced with $p^{(2)}$ and ξ will be replaced with $\xi^{(2)}$, and, for the P2-waves, p will be replaced with $p^{(3)}$ and ξ will be replaced with $\xi^{(3)}$.

With equations 38, 41, 46, and 49, we find for all three Biot waves that their limiting dissipation factors only depend on the complex shear modulus G of the solid frame and are equal to $-\mathrm{Im}(G)/\mathrm{Re}(G)$ and $-2\,\mathrm{Im}(G)/\mathrm{Re}(G)$ for the definitions of Q_V^{-1} and Q_T^{-1}, respectively.

REDUCED FORM OF EXPRESSION FOR THE DISSIPATION FACTORS IN A VISCOELASTIC MATERIAL

In this section, the Q^{-1} formulas in the previous section will be reduced to the dissipation factors in viscoelastic materials, denoted as $\breve{Q}^{-1}$ with an over arc on the symbol Q^{-1}. The homogeneous formulas of $\breve{Q}^{-1}$ should be the same as the well-known formulas of viscoelastic materials, which thus provide a validation of the correctness of the Q^{-1} formulas we derive for effective Biot materials.

The fluid bulk modulus K^f (equation 2) is set as zero, which leads to

$$M \to 0. \tag{50}$$

Then, the viscosity of the fluid is set as infinity $\eta \to \infty$, which leads to

$$\tilde{\rho} \to \infty, \xi \to 0. \tag{51}$$

With the viscoelastic assumptions (i.e., equations 50 and 51) and ignoring the energy related to fluid flux $\mathbf{w}$, the wave equation 1 is reduced to its viscoelastic wave version:

$$[(\breve{H} - G)\nabla\nabla + (G\nabla^2 + \omega^2\rho)\mathbf{I}] \cdot \mathbf{u} = 0. \tag{52}$$

It is well known that the corresponding slownesses for the S- and P-waves are given as

$$\breve{p}^{(1)} = \sqrt{\rho/G},\ \breve{p}^{(2)} = \sqrt{\rho/\breve{H}},\ \breve{H} = K^d + 4G/3. \tag{53}$$

Here, the top arc "˘" again represents the quantities for viscoelastic (as opposed to effective Biot) materials.

Using equations 17 and 19 with $\eta \to \infty$, we easily can derive

$$|\xi|^2 \mathrm{Im}(\tilde{\rho}) \to 0. \tag{54}$$

With the assumptions (equations 50, 51, and 54), the $\breve{Q}^{-1}$ formulas for viscoelastic materials are easily obtained from the corresponding Q^{-1} formulas of the effective Biot materials.

The terms $\breve{Q}_{\mathrm{SV}}^{-1}$ and $\breve{Q}_{\mathrm{SV}H}^{-1}$ are obtained from equations 36 and 37, respectively:

$$\breve{Q}_{\mathrm{SV}}^{-1} = \breve{Q}_{\mathrm{SV}H}^{-1} = -\mathrm{Im}(G)/\mathrm{Re}(G). \tag{55}$$

It is noteworthy that $\breve{Q}_{\mathrm{SV}}^{-1}$ is equal to the corresponding limiting dissipation factor discussed previously. Therefore, $\breve{Q}_{\mathrm{SV}}^{-1}$ is independent of the degree of SV-waves inhomogeneity (i.e., D) for viscoelastic materials.

From equations 39 and 40, $\breve{Q}_{ST}^{-1}$ and $\breve{Q}_{STH}^{-1}$ are obtained as

$$\breve{Q}_{ST}^{-1} = \frac{-2(4D^2|p^2+D^2|+|p^2+2D^2|^2)\mathrm{Im}(G)}{\{\rho(|p^2+D^2|+D^2)+(4D^2|p^2+D^2|+|p^2+2D^2|^2)\mathrm{Re}(G)\}} \tag{56}$$

and

$$\breve{Q}_{STH}^{-1} = -2|p^2|\mathrm{Im}(G)/\{\rho + |p^2|\mathrm{Re}(G)\}. \tag{57}$$

By equation 56, it is easy to find that, unlike the case of $\breve{Q}_{\mathrm{SV}}^{-1}$, quantity $\breve{Q}_{ST}^{-1}$ is dependent on the degree of the SV-wave inhomogeneity. Equations 56 and 57 are exactly same as equations 39 and 40, respectively, of Liu et al. (2020), although they are derived independently.

Based on equations 43 and 44, VI_{P} and VR_{P} are defined as $VI_{\mathrm{P1}}(\xi = 0)$ and $VR_{\mathrm{P1}}(\xi = 0)$, respectively, that is

$$VI_{\mathrm{P}} = 4D^2|p^2 + D^2|\mathrm{Im}(G) + [D^4 + |p^2 + D^2|^2]\mathrm{Im}(\breve{H}) - 2D^2[\mathrm{Re}(p^2) + D^2]\mathrm{Im}(\lambda), \tag{58}$$

$$VR_{\mathrm{P}} = 4D^2|p^2 + D^2|\mathrm{Re}(G) + [D^4 + |p^2 + D^2|^2]\mathrm{Re}(\breve{H}) - 2D^2[\mathrm{Re}(p^2) + D^2]\mathrm{Re}(\lambda). \tag{59}$$

The terms $\breve{Q}_{\mathrm{PV}}^{-1}$ and $\breve{Q}_{\mathrm{PV}H}^{-1}$ are obtained from equations 42 and 45, respectively, as

$$\breve{Q}_{\mathrm{PV}}^{-1} = -VI_{\mathrm{P}}/VR_{\mathrm{P}}, \tag{60}$$

$$\breve{Q}_{\mathrm{PV}H}^{-1} = -\mathrm{Im}(\breve{H})/\mathrm{Re}(\breve{H}). \tag{61}$$

Equations 60 and 61 are equivalent to equations 30 and 32, respectively, of Liu et al. (2020), although they are derived independently.

Then, in a similar manner using equations 47 and 48, we obtain

$$\breve{Q}_{\mathrm{P}T}^{-1} = -2VI_{\mathrm{P}}/\{(|p^2 + D^2| + D^2)[\rho] + VR_{\mathrm{P}}\}, \tag{62}$$

$$\breve{Q}_{\mathrm{P}TH}^{-1} = -2|p^2|\mathrm{Im}(\breve{H})/\{\rho + |p^2|\mathrm{Re}(\breve{H})\}. \tag{63}$$

Equations 62 and 63 are exactly the same as equations 31 and 33, respectively, of Liu et al. (2020), although once again they are derived independently.

It is important to note that equations 38, 41, 46, and 49 of the limiting dissipation factors $Q^{-1}(D = \infty)$ of the poroviscoelastic materials hold true for their viscoelastic counterparts considered as a special case. The dissipation factors $\breve{Q}_{\mathrm{SV}H}^{-1}$ and $\breve{Q}_{\mathrm{PV}H}^{-1}$ in equations 55 and 61 are well known for viscoelastic materials under the definition of Q_V^{-1}. The dissipation factors $\breve{Q}_{\mathrm{ST}H}^{-1}$ and $\breve{Q}_{\mathrm{PT}H}^{-1}$ in equations 57 and 63 easily can be proven to be equal to $2\,\mathrm{Im}(\sigma_{\mathrm{P}})/\mathrm{Re}(\sigma_{\mathrm{P}})$ and satisfy the well-known value $2\alpha v/\omega$ (see section 1 and Appendix B of Liu et al., 2020). The fact that the reduced expressions (to viscoelastic formulas) of the $\breve{Q}^{-1}$ values from the poroviscoelastic formulas in this research are exactly the same as those directly derived from the viscoelastic formulas in Liu et al. (2020) strongly supports the correctness of the Q^{-1} expressions developed in this paper.

NUMERICAL EXAMPLES

The example material that we use in this section for numerical computations is a homogeneous water-filled effective Biot medium that is very similar to sample material A in Liu et al. (2018). In this material, the relaxed bulk modulus and the shear modulus are frequency dependent. A single fractional Zener element (i.e., the Cole-Cole model) can satisfactorily represent the frequency dependence for this material. For the sake of completeness, the material properties are listed in Table 1, along with the parameters of the Cole-Cole model — τ_σ,τ_ε,α — which represent the relaxation times of stress and strain and the fractional derivative order of the fractional Zener element (see equation 3 for $\mathrm{L_Z} = 1$). The superscripts of the Cole-Cole model parameters G and Kd in Table 1 refer to the frequency-dependent shear modulus $G(\omega)$ and the frequency-dependent bulk

modulus $K^d(\omega)$. The relaxed velocities of this material are $V_P0 = 3072$ (m/s), $V_S0 = 1606$ (m/s) for the P1- and S-waves, respectively.

To calculate Q^{-1} with our stipulated approach, the degree of wave inhomogeneity D must be assigned. Here, D has the units of slowness. Theoretically speaking, the range of D is $(-\infty, +\infty)$. For the effective Biot materials, we suggest using a normalized version of D whereby it is divided by the unrelaxed slowness (inverse phase velocity v^{phy} at $\omega = \infty$):

$$D = \hat{D}\,\mathrm{Re}(\sigma[\omega = \infty]) = \hat{D}/v^{\text{phy}}(\omega = \infty). \qquad (64)$$

The reason to choose the unrelaxed slowness rather than the relaxed slowness to normalize D is that the phase velocity v^{phy} of the P2-waves tends to zero at $\omega = 0$ and may cause instabilities (see equation 64).

Figure 1 shows the dispersion curves and dissipation factors of homogeneous S- and P1-waves in the effective Biot material and the classic Biot material given in Table 1. There are two energy dissipation mechanisms, the inner flow model and the Biot global model in the effective Biot theory. With the upscaled poroviscoelastic model (Liu et al., 2018) from the effective Biot model (Pride et al., 2004) the S-waves and P1-waves show very strongly dispersive phase velocities (and high dissipation factors) from the seismic frequency band up to the ultrasonic frequency range, as observed in subsurface reservoir studies. The classic Biot model (Biot, 1956a, 1956b, 1962a, 1962b) has only one (i.e., Biot global) energy dissipation mechanism, which shows its dissipation peak around a frequency of 1.0 E + 6 Hz, that is, the Biot relaxation frequency that separates the viscous-force-dominated flow from the inertial-force-dominated flow (Biot, 1962a, 1962b; Pride et al., 2004). Figure 1 shows that effective Biot theory can correctly describe the high-level dissipation observed in natural reservoirs. That is the reason we choose it in our research.

Figure 1a shows the S-wave phase velocities v_S^{eB} and v_S^{cB} for an effective Biot material (denoted with superscript eB) and a classic Biot material (denoted with superscript cB). Figure 1b shows the P1-wave phase velocities v_{P1}^{eB} and v_{P1}^{cB}. Compared with the v_{P1}^{eB} curve, the dispersion curve v_{P1}^{cB} of the classic Biot theory has minimal frequency dependence.

In Figure 1c, the solid line $1/Q_{SV,T}^{eB}$ shows the S-wave dissipation factors $1/Q_{SV}^{eB}$ and $1/Q_{ST}^{eB}$ under the definition of Q_V^{-1} and Q_T^{-1}, respectively. For the effective Biot material and the homogeneous waves, they are almost identical. The "dashed" line $1/Q_{SV,T}^{cB}$ shows the attenuation curves $1/Q_{SV}^{cB}$ and $1/Q_{ST}^{cB}$ for the classic Biot material, and the homogeneous waves having negligible difference. The $1/Q^{eB}$ of the effective Biot model clearly has two dissipation peaks, the very broad one corresponding to the inner flow mechanism that is superposed with the high-frequency one denoted with a "*" sign corresponding to the Biot global flow mechanism (Biot, 1956a, 1956b, 1962a, 1962b). For the sake of convenience, the two peaks are called the inner flow peak and the Biot flow peak,

Table 1. Material properties of the sample rocks and fluids.

	Parameter	Water
Grains and fluid	K^f (N m^{-2})	2.3E + 9
	ρ^f (kg m^{-3})	1000
	η^f (N m^{-2})	0.001
	Parameter	**Grains**
	K^g (N m^{-2})	3.9E + 10
	ρ^g (kg m^{-3})	2650
	Parameter	**Material**
Solid frame	K^d (N m^{-2})	7.8E + 9 ($\omega = 0$)
	G (N m^{-2})	5.94E + 9 ($\omega = 0$)
	ϕ	0.21
	κ (m^2)	1.03 E-14
	T	$T = 0.5(1 + 1/\phi)$
Cole-Cole model parameters for material		**Shear modulus**
	τ_σ^G (s)	$2\pi \times$ 4.08E-5
	τ_ε^G (s)	$2\pi \times$ 5.19E-5
	α^G	0.527
		Bulk modulus
	τ_σ^{Kd} (s)	$2\pi \times$ 2.68E-5
	τ_ε^{Kd} (s)	$2\pi \times$ 1.90E-4
	α^{Kd}	0.505

respectively, in this paper. Please note that $1/Q^{cB}$ of the classic Biot model exhibits only the Biot flow dissipation peak. Figure 1d shows the P1-wave dissipation factors $1/Q^{eB}_{\mathrm{P1}V}$ and $1/Q^{eB}_{\mathrm{P1}T}$ denoted by the solid line $1/Q^{eB}_{\mathrm{P1}V,T}$ and $1/Q^{cB}_{\mathrm{P1}V}$ and $1/Q^{cB}_{\mathrm{P1}T}$ denoted by the dashed line $1/Q^{cB}_{\mathrm{P1}V,T}$ in a manner similar to Figure 1c. But the Biot global dissipation peaks in the four curves are very tiny (concentrated around the frequency axis and denoted with the "*" sign).

Figure 2 shows the phase velocity dispersion curves and dissipation factors of the homogeneous P2-waves in the effective Biot material and the classic Biot material given in Table 1. Figure 2a shows the P2-wave phase velocities v^{eB}_{P2} and v^{cB}_{P2} for the effective Biot material (denoted with superscript eB) and the classic Biot material (denoted with superscript cB); Figure 2b shows the corresponding P2-wave dissipation factors of $1/Q^{eB}_{\mathrm{P2}T}$ and $1/Q^{cB}_{\mathrm{P2}T}$ under the definition of Q_T^{-1} as well as $1/Q^{eB}_{\mathrm{P2}V}$ and $1/Q^{cB}_{\mathrm{P2}V}$ under the definition Q_V^{-1} with their ordinate values given on the right side. Figure 2a shows that the effective Biot P2-wave phase velocity has dispersion features very similar to its classic Biot counterpart. The inner flow dissipation mechanism does not cause much difference on the P2-waves, especially for low frequencies, that is, less than the Biot relaxation frequency. This fact is well-represented by the dissipation factor curves $1/Q^{eB}_{\mathrm{P2}T}$ and $1/Q^{cB}_{\mathrm{P2}T}$ under the definition of Q_T^{-1} (see the solid line and the "dotted" line). However, the curves $1/Q^{eB}_{\mathrm{P2}V}$ and $1/Q^{cB}_{\mathrm{P2}V}$ under the definition Q_V^{-1} show apparently inadmissible results. The $1/Q^{cB}_{\mathrm{P2}V}$ curve for the classic Biot material has extremely high values ($\gg 500$) in the low-frequency range, whereas $1/Q^{eB}_{\mathrm{P2}V}$ even has negative values (see their y-axis on the right side of the figure). The physical meaning behind this observation is that a P2-wave is more like a diffusive mode at low frequency in which the real part of the complex modulus Re(Z) tends to be zero and the imaginary and real parts of the of the complex velocity are of comparable size (Berryman and Wang, 2000). Thus, as we have stated, Berryman and Wang (2000) use the definition $Q^{-1}=2\alpha v/\omega$ in all cases, by which the Q^{-1} of a P2-wave is calculated to be near 2 (for the low frequency, similar to our Q_T^{-1} values). For a better understanding of this phenomenon, we investigate the dissipation factors of homogeneous diffusive waves in Appendix D. It is worth mentioning again that the definition $Q^{-1}=2\alpha v/\omega$ is strictly only valid under the assumption of homogeneous waves.

Figure 3 is a partial enlargement of Figure 2 in the frequency range from 1.75E5 to 1.0E7 Hz. From this figure, we find that, as the frequency exceeds the Biot relaxation frequency, for the homogeneous S-waves and the P1-waves, the dissipation factor curves under the definition of Q_T^{-1} and Q_V^{-1} have a negligible difference for either an effective Biot material or a classic material. In the high-frequency range, the P2 wave gradually transforms from a diffusive wave to a propagative wave. In a subsequent section, we will investigate how the degree of the inhomogeneity of the wave affects Q_{P2}^{-1}.

Figure 4 shows the dispersion curves and dissipation factors of inhomogeneous S-waves in the effective Biot material given in Table 1. Phase velocities (Figure 4a) increase with increasing frequency and decrease with increasing inhomogeneity parameter D, as expected. Similar to what is observed in Figure 1c, the dissipation

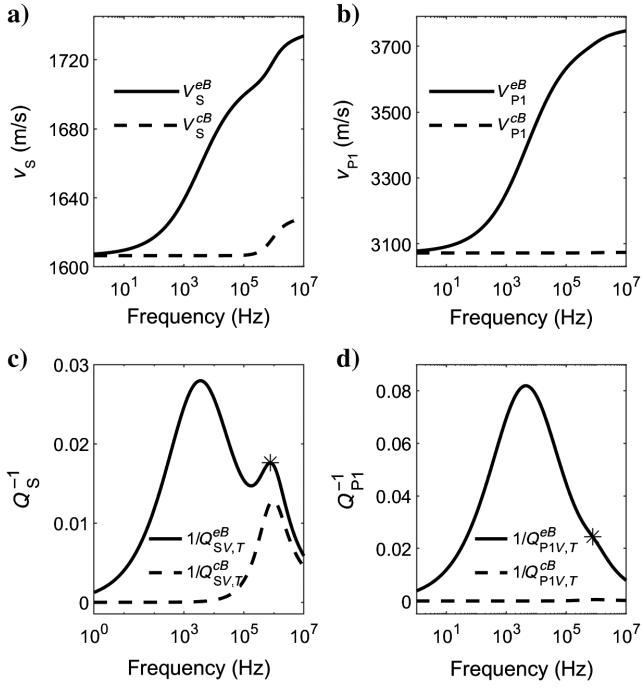

Figure 1. Dispersion curves and dissipation factors of homogeneous waves for the effective Biot material and classic Biot material given in Table 1: (a) S-wave phase velocities v^{eB}_{S} and v^{cB}_{S} for effective Biot material (denoted with superscript eB) and classic Biot material (denoted with superscript cB), respectively; (b) P1-wave phase velocities v^{eB}_{P1} and v^{cB}_{P1}; (c) S-wave dissipation factors of $1/Q^{eB}_{SV}$ and $1/Q^{eB}_{ST}$ under the definition of Q_V^{-1} and Q_T^{-1}, respectively, for effective Biot material are identical and denoted by $1/Q^{eB}_{SV,T}$, $1/Q^{cB}_{SV}$, and $1/Q^{cB}_{ST}$ classic Biot material are identical and denoted by $1/Q^{cB}_{SV,T}$; (d) in a manner similar to (c), P1-wave dissipation factors $1/Q^{eB}_{\mathrm{P1}V}$ and $1/Q^{eB}_{\mathrm{P1}T}$ are denoted by $1/Q^{eB}_{\mathrm{P1}V,T}$, and $1/Q^{cB}_{\mathrm{P1}V}$ and $1/Q^{cB}_{\mathrm{P1}T}$ are denoted by $1/Q^{cB}_{\mathrm{P1}V,T}$. The "star" symbols in (c and d) indicate the frequencies of Biot dissipation peaks. Note that in (c and d) the two curves for Q_V^{-1} and Q_T^{-1} are identical in each case of a classic and an effective Biot material.

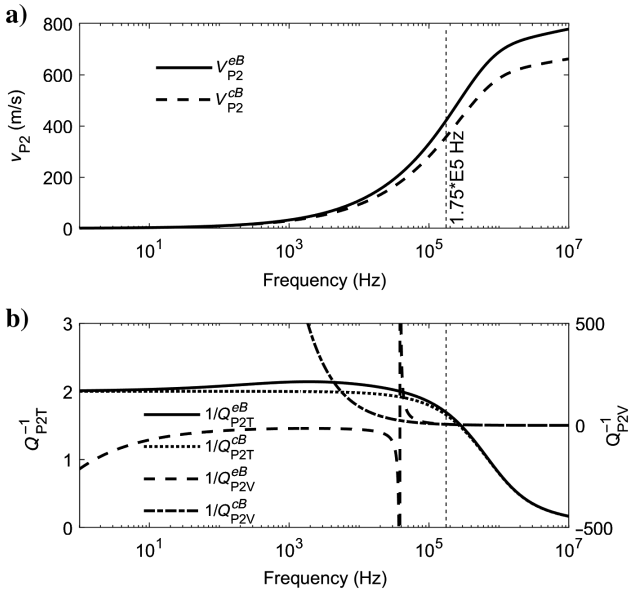

Figure 2. Dispersion curves and dissipation factors of P2-homogeneous waves for the effective Biot material and classic Biot material given in Table 1: (a) P2-wave phase velocities, v^{eB}_{P2} and v^{cB}_{P2}, for effective Biot material (denoted with superscript eB) and classic Biot material (denoted with superscript cB) and (b) P2-wave dissipation factors of $1/Q^{eB}_{\mathrm{P2}T}$ and $1/Q^{cB}_{\mathrm{P2}T}$ under the definition of Q_T^{-1}; $1/Q^{eB}_{\mathrm{P2}V}$ and $1/Q^{cB}_{\mathrm{P2}V}$ under the definition Q_V^{-1} with the right-side y-axis.

factor diagrams under the definition of Q_T^{-1} (Figure 4b), Q_{ST}^{-1}, shows two dissipation peaks (corresponding to the inner flow and Biot flow mechanisms) for smaller values of D. But it is interesting to see that, with increasing D, the two dissipation peaks have opposite trends, the contribution to Q_{ST}^{-1} by the Biot flow decreases (see the smaller peak denoted with Biot flow) whereas the contribution to Q_{ST}^{-1} from the inner flow mechanisms increases (see the very broad and larger peak denoted with inner flow). This phenomenon can be explained easily by our limiting dissipation factor expression $Q_{ST}^{-1}(D=\infty) = -2\,\mathrm{Im}(G)/\mathrm{Re}(G)$ (see equation 41). For the homogeneous SV-waves ($D=0$), the Q_{ST}^{-1} dispersion contributed by inner flow (so denoted) tends to the dispersion of the shear modulus, that is, $-\mathrm{Im}(G)/\mathrm{Re}(G)$ (see equations 16 and 40). With increasing D, Q_{ST}^{-1} tends to go up to its limiting dissipation factor $-2\,\mathrm{Im}(G)/\mathrm{Re}(G)$. But, in the frequency range of the Biot-flow dissipation peak, the value of $-2\,\mathrm{Im}(G)/\mathrm{Re}(G)$ is below the homogeneous Q_{ST}^{-1} because of superposition of the contribution from Biot flow. Therefore, the Biot-flow peak tends to disappear with increasing D. In summary, the dissipation factors of S-waves tend to monotonically change from their homogeneous dissipation factor values towards their limiting dissipation factor values.

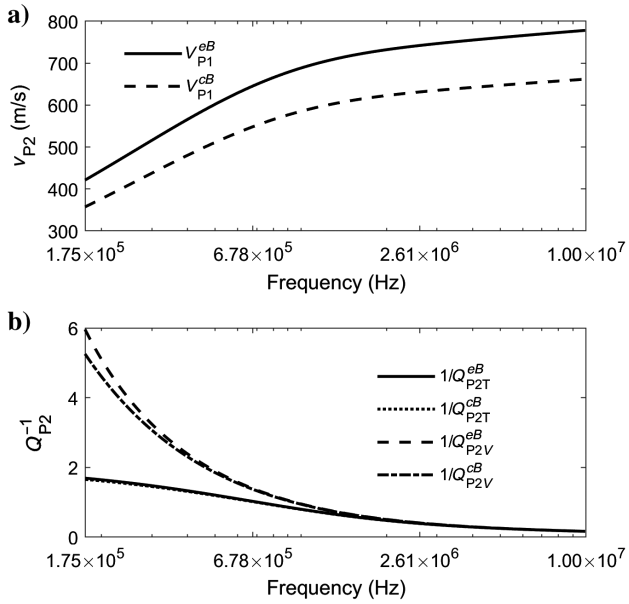

Figure 3. Partial enlargement of Figure 2 in the frequency range from 1.75×10^5 to 1.0×10^7 Hz.

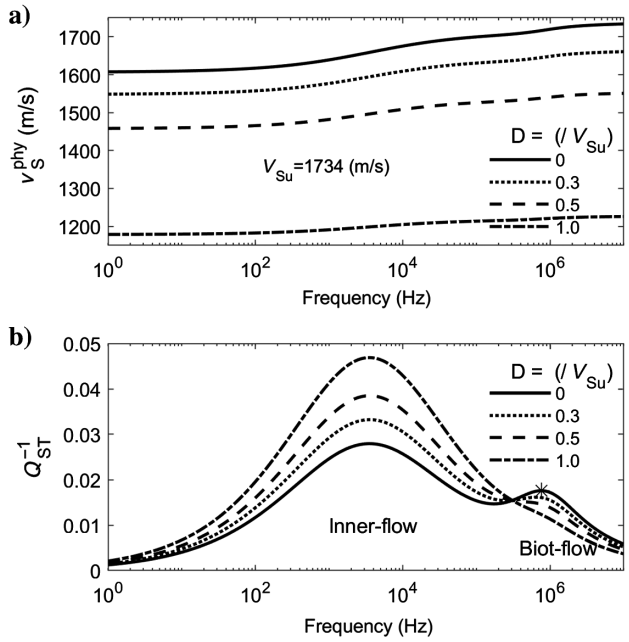

Figure 4. Dispersion curves and dissipation factors of inhomogeneous S-waves for effective Biot material given in Table 1. (a) Phase velocities and (b) dissipation factors under the definition of Q_T^{-1} are given at different D values. The two dissipation peaks correspond to the inner flow and Biot flow dissipation mechanisms. The star * signs (the lower plot) indicate the Biot flow dissipation peak.

Figure 5 presents a comparison between Q_V^{-1} and Q_T^{-1} of S-waves, denoted as Q_{SV}^{-1} and Q_{ST}^{-1}, at different values of the inhomogeneity parameter D. Although Q_{ST}^{-1} of the inner flow peak increases with increasing D, its Q_{SV}^{-1} counterpart is almost independent of D (see the circle sign as the peak point). This can be explained from equation 36. At a frequency around the inner flow peak, the $\mathrm{Im}(\tilde{\rho})$ term has a very small value and equation 36 tends to equal its homogeneous wave version, that is, equation 55 that is already the limiting dissipation factor $Q_{SV}^{-1}(D=\infty)$ and is totally independent of D. But Q_{ST}^{-1} trends up to its limiting dissipation factor that is double the current value of Q_{SV}^{-1} with increasing D. Thus, difference between Q_{SV}^{-1} and Q_{ST}^{-1} significantly increases with

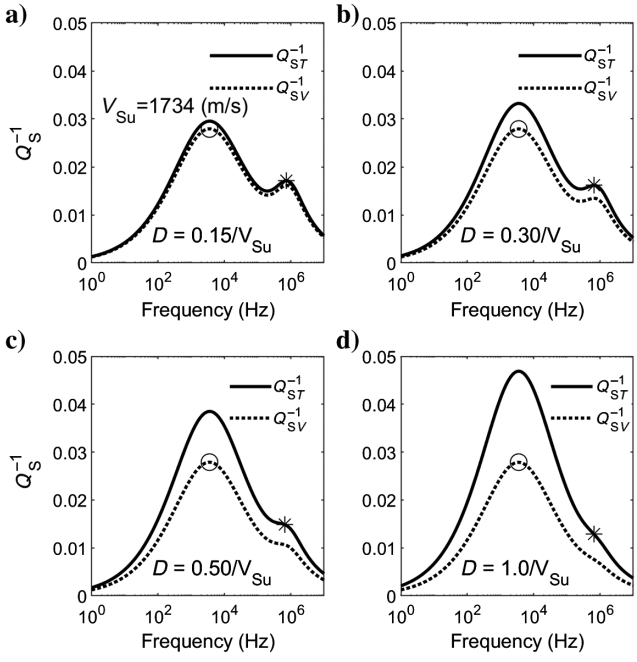

Figure 5. Comparison between Q_V^{-1} and Q_T^{-1} of S-waves for the effective Biot material given in Table 1 at different D values: (a) $D=0.15/V_{Su}$, (b) $D=0.3/V_{Su}$, (c) $D=0.5/V_{Su}$, and (d) $D=1.0/V_{Su}$. The "circle" symbol indicates an almost-constant Q_{SV}^{-1} peak of 0.028 at frequency of 3512 Hz. The "star" symbol indicates the frequencies of Biot global flow dissipation peaks.

increasing D. We can draw the same conclusions as we did for Figure 4.

In Figure 6, we show the dispersion curves and dissipation factors of inhomogeneous P1-waves in the effective Biot material given in Table 1. Phase velocities (Figure 6a) increase with increasing frequency and decrease with increasing inhomogeneity parameter D, as expected. The dissipation factor plots (Figure 6b) under the definition of Q_T^{-1}, that is, Q_{P1T}^{-1}, decrease with increasing D. This seems contradictory to Borcherdt and Wennerberg (1985) and also is reported by Liu et al. (2020) for viscoelastic materials. This phenomenon can also be easily explained by our limiting dissipation factor $Q_{P1T}^{-1}(D=\infty) = -2\mathrm{Im}(G)/\mathrm{Re}(G)$ (equation 49). The homogeneous P1-waves in the sample material are roughly three times more dissipative than the homogeneous S-waves (see Figure 1c and 1d). With increasing D, Q_{P1T}^{-1} tends to go down to its limiting dissipation factor $-2\,\mathrm{Im}(G)/\mathrm{Re}(G)$ or is twice as dissipative as the homogeneous S-waves.

Figure 7 shows the comparison between Q_V^{-1} and Q_T^{-1} for P1-waves, denoted as Q_{P1V}^{-1} and Q_{P1T}^{-1}, respectively, for different values of the wave inhomogeneity parameter D. The terms Q_{P1V}^{-1} and Q_{P1T}^{-1} decrease with increasing D as depicted in Figure 6. The Biot peak of the P1-wave is very small in this example. But the difference between Q_{P1V}^{-1} and Q_{P1T}^{-1} becomes significant with increasing D (see Figure 7c and 7d) for strongly dissipative media (see the difference around the dissipation factor peak). The reason is that Q_{P1V}^{-1} tends to go down to its limiting dissipation factor $-\mathrm{Im}(G)/\mathrm{Re}(G)$ (equation 46) whereas Q_{P1T}^{-1} tends to $-2\mathrm{Im}(G)/\mathrm{Re}(G)$ (equation 49). In summary, the dissipation factors of P1-waves tend to change from their homogeneous wave dissipation factor values and finally satisfy their limiting dissipation factor values.

The dispersion curves and dissipation factors of inhomogeneous P2-waves are depicted in Figure 8 for the effective Biot material given in the Table 1. Phase velocities (Figure 8a) increase with increasing frequency and decrease with increasing values of the wave

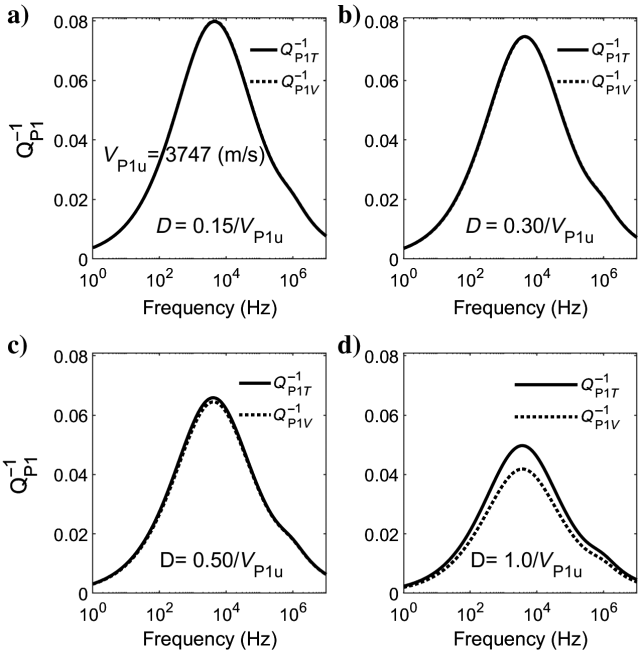

Figure 7. Comparison between Q_V^{-1} and Q_T^{-1} of P1-waves for the effective Biot material given in Table 1 at different D values: (a) $D = 0.15/V_{P1u}$, (b) $D = 0.3/V_{P1u}$, (c) $D = 0.5/V_{P1u}$, and (d) $D = 1.0/V_{P1u}$.

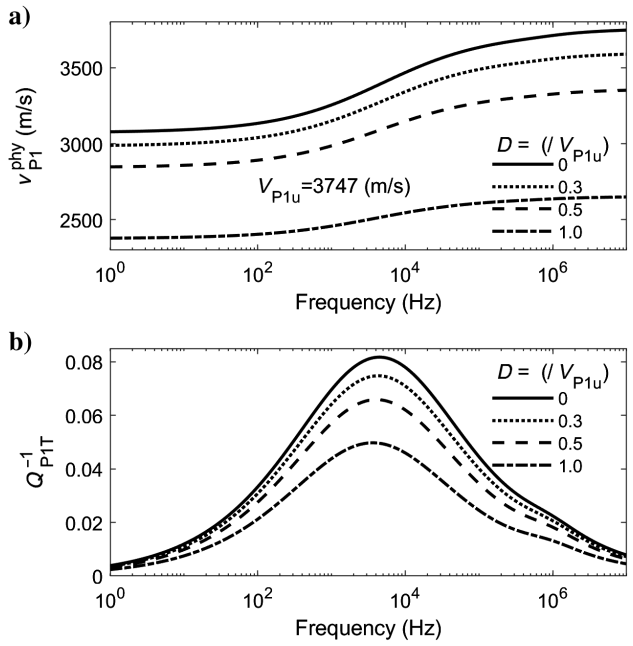

Figure 6. Dispersion curves and dissipation factors of inhomogeneous P1-waves for the effective Biot material given in Table 1. (a) The phase velocities and (b) dissipation factors under the definition of Q_T^{-1} are given at different D values.

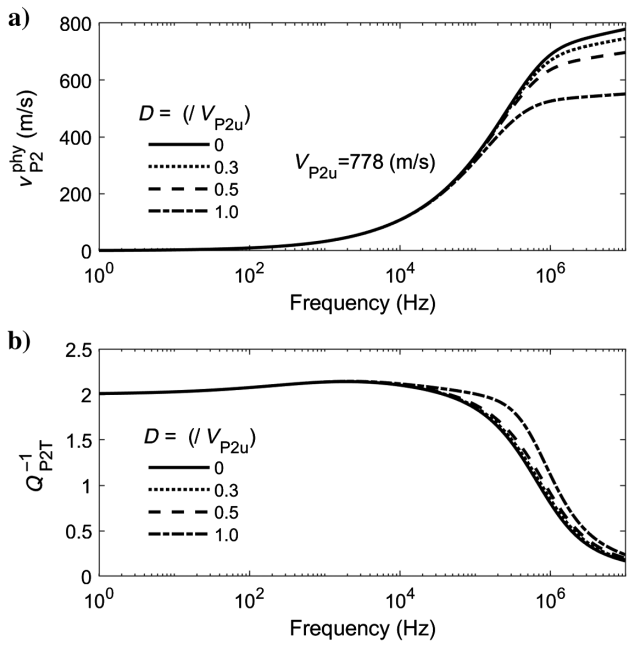

Figure 8. Dispersion curves and dissipation factors of inhomogeneous P2-waves for the effective Biot material given in the Table 1. (a) The phase velocities and (b) dissipation factors under the definition of Q_T^{-1} are given at different D values.

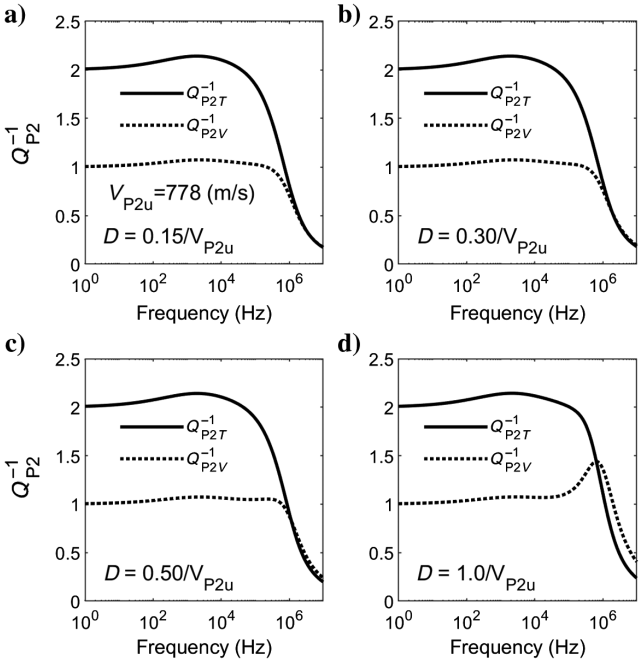

Figure 9. Comparison between Q_V^{-1} and Q_T^{-1} of P2-waves in the effective Biot material given in Table 1 at different D values: (a) $D = 0.15/V_{P2u}$, (b) $D = 0.3/V_{P2u}$, (c) $D = 0.5/V_{P2u}$, and (d)$D = 1.0/V_{P2u}$.

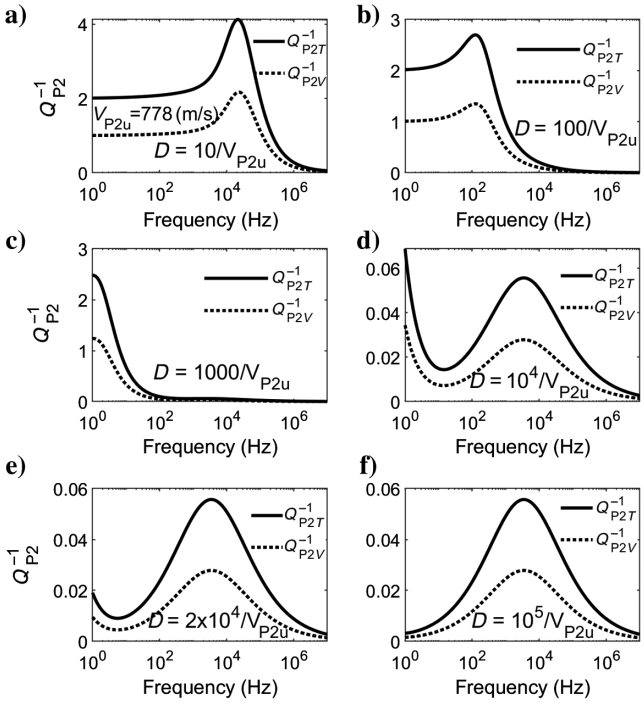

Figure 10. Comparison between Q_V^{-1} and Q_T^{-1} of P2-waves in the effective Biot material given in Table 1 at different D values: (a) $D = 10/V_{P2u}$, (b) $D = 100/V_{P2u}$, (c) $D = 1000/V_{P2u}$, (d) $D = 10^4/V_{P2u}$, (e) $D = 2.0 \times 10^4/V_{P2u}$, and (f) $D = 10^5/V_{P2u}$.

inhomogeneity parameter D, as expected. The dissipation factor diagrams (Figure 8b) under the definition of Q_T^{-1} change very slowly with increasing D. By contrast, Q_{P2T}^{-1} remains at or slightly above the value 2 for the frequency range up to about 10E5 Hz. This high dissipation factor means the P2-wave cannot be a propagative wave (Berryman and Wang, 2000).

Figure 9 shows the comparison between Q_V^{-1} and Q_T^{-1} for the P2-waves, denoted as Q_{P2V}^{-1} and Q_{P2T}^{-1}, at different inhomogeneity parameter D values. We find that even at small values of inhomogeneity, for example, D =0.15/778 (s/m) in Figure 9a, the inadmissible case for Q_{P2V}^{-1} is avoided, unlike in Figure 2b. Similar to Figure 8b, Q_{P2V}^{-1} and Q_{P2T}^{-1} change very slowly with increasing D. However, the Q_{P2V}^{-1} and Q_{P2T}^{-1} curves seem to be disconnected with their limiting dissipation factors (dependent on the complex shear modulus). This question will be investigated in calculations which will be shown in the following section for Figure 10.

Figure 10 presents a comparison of Q_{P2V}^{-1} and Q_{P2T}^{-1} at large D values of [1.0 E + 1 to 1.0 E + 5]/778 (s/m). Figure 10a shows the diagrams for D = 10/778. There is a relatively narrow dissipation peak (Biot flow-type peak) for each of the two dissipation curves at frequencies slightly higher than 1.0 E + 4 Hz. Actually the peak also occurs in the Q_{P2V}^{-1} curve in Figure 9d at the Biot flow peak frequency range of the homogeneous wave. The physical mechanism creating this dissipation peak is not at all clear. However, in Figure 10b–10f, with D increasing, this narrow dissipation peak shifts to lower frequency values and gradually disappears whereas the dissipation peaks of the limiting dissipation factors of Q_{P2V}^{-1} and Q_{P2T}^{-1} gradually become more pronounced. In Figure 10f, we find that Q_{P2T}^{-1} is roughly two times larger than Q_{P2V}^{-1} over the full frequency range, satisfying the limiting dissipation factors equations 46 and 49. Somewhat surprisingly, the limiting dissipation factors only depend on the complex shear modulus for all three Biot waves.

CONCLUSION

In this study, explicit expressions for the dissipation factors Q^{-1} of inhomogeneous S-waves, P1-waves, and P2-waves are derived in isotropic poroviscoelastic media under the two differing definitions of Q_V^{-1} and Q_T^{-1}. These Q^{-1} expressions are given as concise and simple functions of the material parameters and the wave inhomogeneity parameter D. The explicit functions provide a direct way to investigate the dependency of these dissipation factors on the degree of wave inhomogeneity. We find that the limiting dissipation factors only depend on the ratio of the imaginary part to the real part of the shear modulus, $-\mathrm{Im}(G)/\mathrm{Re}(G)$, for all three Biot waves: SV, fast P, and slow P. These results are used successfully to explain and describe how these dissipation factors depend on the wave inhomogeneity D.

We reduce our explicit Q^{-1} formulas from the poroviscoelastic model to the viscoelastic model as a special case. These reduced viscoelastic formulas are the same as their counterparts of previously published results, although they are derived independently and provide an extra check on the correctness of our results.

The limiting dissipation factors are defined as $Q^{-1}(D = \infty)$ for which the condition $D = \infty$ means the corresponding phase velocities are zero according to equations 8 and 9. It is difficult to imagine these "propagative waves" exist in a physical sense. But, the Biot flow type peaks occurring in Figure 10 and that shift toward lower frequency with increasing D must have some physical explanation. We leave this question for further investigation.

ACKNOWLEDGMENTS

We are grateful to the College of Petroleum Engineering & Geosciences, King Fahd University of Petroleum and Minerals, Kingdom of Saudi Arabia (SF18066), for supporting this research. We are indebted to editor J. Shragge, assistant editors C. Farquharson and S. Hestholm, and three anonymous reviewers for constructive comments that have improved the clarity and content of our manuscript.

DATA AND MATERIALS AVAILABILITY

This is a theoretical paper and no real data was used in the study.

APPENDIX A

ELASTICITY MATRIX AND GENERALIZED DENSITY MATRIX FOR ISOTROPIC POROUS MEDIA

For an inhomogeneous wave propagating in the x-z plane, the extended strain vector is written as

$$\mathbf{e} = (e_1, 0, e_3, 0, e_5, 0, -\zeta)^T. \tag{A-1}$$

Based on the elasticity matrix of the undrained porous medium in Carcione (2014), we write the elasticity matrix $\mathbf{P}$ for the isotropic poroviscoelastic media in terms of the Biot elastic moduli as

$$\mathbf{P} = \begin{pmatrix} H & \lambda & \lambda & 0 & 0 & 0 & C \\ \lambda & H & \lambda & 0 & 0 & 0 & C \\ \lambda & \lambda & H & 0 & 0 & 0 & C \\ 0 & 0 & 0 & G & 0 & 0 & 0 \\ 0 & 0 & 0 & 0 & G & 0 & 0 \\ 0 & 0 & 0 & 0 & 0 & G & 0 \\ C & C & C & 0 & 0 & 0 & M \end{pmatrix}, \quad \begin{cases} H = K^{\mathrm{sat}} + 4G/3 \\ K^{\mathrm{sat}} = K^d + \alpha^2 M \\ C = \alpha M \\ \lambda = H - 2G \end{cases}. \tag{A-2}$$

The general density matrix $\mathbf{R}$ and extended stress matrix $\sum$ (with entries of averaged stress s_{ij} $i, j = 1,2,3$ and pore pressure p_f) (Carcione, 2014) are written as

$$\mathbf{R} = \begin{pmatrix} \rho & 0 & 0 & \rho_f & 0 & 0 \\ 0 & \rho & 0 & 0 & \rho_f & 0 \\ 0 & 0 & \rho & 0 & 0 & \rho_f \\ \rho_f & 0 & 0 & \tilde{\rho}(\omega) & 0 & 0 \\ 0 & \rho_f & 0 & 0 & \tilde{\rho}(\omega) & 0 \\ 0 & 0 & \rho_f & 0 & 0 & \tilde{\rho}(\omega) \end{pmatrix}, \quad \sum = -\frac{1}{2} \begin{pmatrix} s_{11} & s_{12} & s_{13} \\ s_{12} & s_{22} & s_{23} \\ s_{13} & s_{23} & s_{33} \\ -p_f & 0 & 0 \\ 0 & p_f & 0 \\ 0 & 0 & p_f \end{pmatrix}^T. \tag{A-3}$$

The complex strain energy density V^c (or $\mathbf{e}^T \cdot \mathbf{P} \cdot \mathbf{e}^*$ in equations 25 or 27) can be written as

$$V^c = \mathbf{e}^{\mathbf{T}} \cdot \mathbf{P} \cdot \mathbf{e}^* = e_1[He_1^* + \lambda e_3^* + C(div\,\mathbf{w})^*] + e_3[\lambda e_1^* + He_3^* + C(div\,\mathbf{w})^*] + e_5 G e_5^* + (div\,\mathbf{w})[Ce_1^* + Ce_3^* + M(div\,\mathbf{w})^*]. \tag{A-4}$$

The complex kinetic energy density T^c (or $\mathbf{v}^{T*} \cdot \mathbf{R} \cdot \mathbf{v}$ in equations 26 or 28) can be written as

$$T^c = \mathbf{v}^{T*} \cdot \mathbf{R} \cdot \mathbf{v} = \omega^2 \begin{pmatrix} \rho u_1^* u_1 + \rho_f u_1^* w_1 + \rho u_3^* u_3 + \rho_f u_3^* w_3 \\ + \rho_f w_1^* u_1 + \tilde{\rho}(\omega) w_1^* w_1 + \rho_f w_3^* u_3 + \tilde{\rho}(\omega) w_3^* w_3 \end{pmatrix}. \tag{A-5}$$

APPENDIX B

STRAIN AND KINETIC ENERGY DENSITIES OF THE S-WAVE

The complex amplitude vector of S-waves is orthogonal to the complex slowness (see equation 16). Using equations 31 and 32, the solid particle displacement components of S-waves are rewritten as

$$u_1 = \sigma A \exp[-\omega(Dx + \mathrm{Im}(\sigma)z)] \exp[i\omega(\mathrm{Re}(\sigma)z - t)]$$
$$u_3 = -iDA \exp[-\omega(Dx + \mathrm{Im}(\sigma)z)] \exp[i\omega(\mathrm{Re}(\sigma)z - t)]. \tag{B-1}$$

S-wave strain energy density

The components of strain array $\mathbf{e}$ for the S-wave are obtained from the equations 23 and 24:

$$e_1 = \partial_1 u_1 = -\omega D\sigma A \exp[-\omega(Dx + \mathrm{Im}(\sigma)z)] \exp[i\omega(\mathrm{Re}(\sigma)z - t)]$$
$$e_3 = \partial_3 u_3 = \omega D\sigma A \exp[-\omega(Dx + \mathrm{Im}(\sigma)z)] \exp[i\omega(\mathrm{Re}(\sigma)z - t)]$$
$$e_5 = \partial_1 u_3 + \partial_3 u_1 = i\omega(D^2 + \sigma^2) A \exp[-\omega(Dx + \mathrm{Im}(\sigma)z)] \exp[i\omega(\mathrm{Re}(\sigma)z - t)]$$
$$\nabla \cdot \mathbf{w} = 0 \tag{B-2}$$

To avoid redundancy, the quadratic terms in equation A-4 are written in the form of a matrix defined as EMES:

$$\mathrm{EMES} = \begin{bmatrix} e_1 H e_1^* & e_1 \lambda e_3^* & e_1 C(\nabla \cdot \mathbf{w})^* \\ e_3 \lambda e_1^* & e_3 H e_3^* & e_3 C(\nabla \cdot \mathbf{w})^* \\ e_5 G e_5^* & 0 & 0 \\ (\nabla \cdot \mathbf{w}) C e_1^* & (\nabla \cdot \mathbf{w}) C e_3^* & (\nabla \cdot \mathbf{w}) M (\nabla \cdot \mathbf{w})^* \end{bmatrix}. \tag{B-3}$$

Substituting equation B-2 into equation B-3, we have

$$\mathrm{EMES} = \omega^2|A|^2 \begin{bmatrix} D^2|p^2+D^2|H & -D^2|p^2+D^2|\lambda & 0 \\ -D^2|p^2+D^2|\lambda & D^2|p^2+D^2|H & 0 \\ |p^2+2D^2|^2G & 0 & 0 \\ 0 & 0 & 0 \end{bmatrix} \times \exp[-2\omega(Dx+\mathrm{Im}(\sigma)z)]. \quad \text{(B-4)}$$

Noting $H = \lambda + 2G$ (see equation A-2), the complex strain energy density of S-wave V_S^c is written as

$$V_1^c = \sum_{i,j} \mathrm{EMES}_{ij} = \omega^2|A|^2(4D^2|p^2+D^2|+|p^2+2D^2|^2)G\exp[-2\omega(Dx+\sigma_I z)]. \quad \text{(B-5)}$$

S-wave kinetic energy density

In a manner similar to EMES, the quadratic terms in equation A-5 are written in the matrix defined as VRVS:

$$\mathrm{VRVS} = \begin{bmatrix} u_1^*\rho u_1 & u_1^*\rho_f w_1 \\ u_3^*\rho u_3 & u_3^*\rho_f w_3 \\ w_1^*\rho_f u_1 & w_1^*\tilde{\rho}(\omega) w_1 \\ w_3^*\rho_f u_3 & w_3^*\tilde{\rho}(\omega) w_3 \end{bmatrix}. \quad \text{(B-6)}$$

Substituting equations B-1 and 29 into equation B-6, we have

$$\mathrm{VRVS} = \omega^2|A|^2 \begin{bmatrix} \rho|p^2+D^2| & \rho_f|p^2+D^2|\xi \\ \rho D^2 & \rho_f D^2\xi \\ \rho_f|p^2+D^2|\xi^* & |\xi|^2|p^2+D^2|\tilde{\rho}(\omega) \\ \rho_f D^2\xi^* & |\xi|^2 D^2\tilde{\rho}(\omega) \end{bmatrix} \times \exp[-2\omega(Dx+\mathrm{Im}(\sigma)z)]. \quad \text{(B-7)}$$

Then, the complex kinetic energy density of S-wave T_S^c is written as

$$T_1^c = \sum_{i,j} VRVS_{ij} = \omega^2|A|^2[\rho+\rho_f 2\mathrm{Re}(\xi)+|\xi|^2\tilde{\rho}(\omega)](|p^2+D^2|+D^2) \times \exp[-2\omega(Dx+\mathrm{Im}(\sigma)z)]. \quad \text{(B-8)}$$

APPENDIX C

STRAIN AND KINETIC ENERGY DENSITIES OF P-WAVES

The complex amplitude vector of P-waves is parallel to the complex slowness (see equation 18). Using equations 31 and 33, the solid particle displacement components are rewritten as

$$\begin{aligned} u_1 &= iAD\ \exp[-\omega(Dx+\mathrm{Im}(\sigma)z)]\exp[i\omega(\mathrm{Re}(\sigma)z-t)] \\ u_3 &= A\sigma\exp[-\omega(Dx+\mathrm{Im}(\sigma)z)]\exp[i\omega(\mathrm{Re}(\sigma)z-t)] \end{aligned}. \quad \text{(C-1)}$$

P-wave strain energy density

The components of strain array **e** for P-wave are obtained from the definitions, that is, equations 23 and 24:

$$\begin{aligned} e_1 &= \partial_1 u_1 = -i\omega AD^2\exp[-\omega(Dx+\mathrm{Im}(\sigma)z)]\exp[i\omega(\mathrm{Re}(\sigma)z-t)] \\ e_3 &= \partial_3 u_3 = i\omega A\sigma^2\exp[-\omega(Dx+\mathrm{Im}(\sigma)z)]\exp[i\omega(\mathrm{Re}(\sigma)z-t)] \\ e_5 &= \partial_1 u_3+\partial_3 u_1 = (-1+i)\omega AD\sigma\exp[-\omega(Dx+\mathrm{Im}(\sigma)z)]\exp[i\omega(\mathrm{Re}(\sigma)z-t)] \\ div\mathbf{w} &= \xi(\partial_1 u_1+\partial_3 u_3) = i\omega A\xi p^2\exp[-\omega(Dx+\mathrm{Im}(\sigma)z)]\exp[i\omega(\mathrm{Re}(\sigma)z-t)] \end{aligned}. \quad \text{(C-2)}$$

To avoid redundancy, we define a matrix EMEP and write the quadratic terms in equation A-4 in matrix form:

$$\mathrm{EMEP} = \begin{bmatrix} e_1 H e_1^* & e_1\lambda e_3^* & e_1 C(\nabla\cdot\mathbf{w})^* \\ e_3\lambda e_1^* & e_3 H e_3^* & e_3 C(\nabla\cdot\mathbf{w})^* \\ e_5 G e_5^* & 0 & 0 \\ (\nabla\cdot\mathbf{w})Ce_1^* & (\nabla\cdot\mathbf{w})Ce_3^* & (\nabla\cdot\mathbf{w})M(\nabla\cdot\mathbf{w})^* \end{bmatrix}. \quad \text{(C-3)}$$

Substituting equation C-2 into equation C-3, we have

$$\mathrm{EMEP} = \omega^2|A|^2 \begin{bmatrix} D^4H & -D^2(p^{2*}+D^2)\lambda & -D^2\xi^* p^{2*}C \\ -D^2(p^2+D^2)\lambda & |p^2+D^2|^2H & \xi^*(p^2+D^2)p^{2*}C \\ 4D^2|p^2+D^2|G & 0 & 0 \\ -D^2\xi p^2 C & \xi p^2(p^{2*}+D^2)C & |\xi p^2|^2 M \end{bmatrix} \times \exp[-2\omega(Dx+\mathrm{Im}(\sigma)z)]. \quad \text{(C-4)}$$

With equation 6, the values of σ^2 have been replaced with p^2+D^2. Then, the complex P-wave strain energy density $V_{\mathrm{P1,P2}}^c$ is written as

$$V_{2,3}^c = \sum_{i,j} \mathrm{EMEP}_{ij} = \omega^2|A|^2 \left\{ \begin{matrix} 4D^2|p^2+D^2|G+[D^4+|p^2+D^2|^2]H \\ -2D^2[\mathrm{Re}(p^2)+D^2]\lambda+2\mathrm{Re}(\xi)|p^2|^2C+|\xi p^2|^2M \end{matrix} \right\} \times \exp[-2\omega(Dx+\mathrm{Im}(\sigma)z)]. \quad \text{(C-5)}$$

Here, the material slowness (of homogeneous waves) p will be replaced with $p^{(2)}$ or $p^{(3)}$ and ξ will be replaced with $\xi^{(2)}$ or $\xi^{(3)}$ corresponding to the subscripts, 2 and 3 of $V^c_{2,3}$, respectively. This also holds true for the following kinetic energy density.

P-wave kinetic energy density

In a manner similar to EMEP, we define matrix VRVP, use equations C-1 and 29, and write the quadratic terms in equation A-5 in matrix form:

$$\mathrm{VRVP} = \omega^2 \begin{bmatrix} u_1^*\rho u_1 & u_1^*\rho_f w_1 \\ u_3^*\rho u_3 & u_3^*\rho_f w_3 \\ w_1^*\rho_f u_1 & w_1^*\tilde{\rho}(\omega) w_1 \\ w_3^*\rho_f u_3 & w_3^*\tilde{\rho}(\omega) w_3 \end{bmatrix} = \omega^2|A|^2 \begin{bmatrix} \rho D^2 & \rho_f D^2\xi \\ \rho|p^2+D^2| & \rho_f|p^2+D^2|\xi \\ \rho_f D^2\xi^* & |\xi|^2 D^2\tilde{\rho}(\omega) \\ \rho_f|p^2+D^2|\xi^* & |\xi|^2|p^2+D^2|\tilde{\rho}(\omega) \end{bmatrix} \times \exp[-2\omega(Dx + \mathrm{Im}(\sigma)z)]. \tag{C-6}$$

Then, the complex P-wave kinetic energy density $T^c_{\mathrm{P1,P1}}$ is written as

$$T^c_{2,3} = \sum_{i,j} VRVP_{ij} = \omega^2|A|^2(|p^2+D^2|+D^2)[\rho + 2\rho_f \mathrm{Re}(\xi) + |\xi|^2\tilde{\rho}(\omega)] \times \exp[-2\omega(Dx + \mathrm{Im}(\sigma)z)]. \tag{C-7}$$

APPENDIX D

DISSIPATION FACTORS OF HOMOGENEOUS DIFFUSION WAVES

The diffusion wave equation with the diffusivity $\tilde{D}$ and without a source term can be written as (e.g., Mandelis, 2000)

$$\Delta u - \frac{1}{\tilde{D}}\partial_t u = 0. \tag{D-1}$$

The corresponding pseudowave equation with complex velocity v^c is

$$\Delta u - \frac{1}{(v^c)^2}\partial_t^2 u = 0. \tag{D-2}$$

Assuming a homogeneous wave with the complex wavenumber $\kappa + i\alpha$, we have

$$u(t,x) = u_0 \exp[i(\kappa + i\alpha)x - i\omega t], \tag{D-3}$$

and substituting equation D-3 into equations D-1 and D-2 produces the complex velocity

$$(v^c)^2 = -i\omega\tilde{D} \quad \text{or} \quad v^c = \pm\frac{1}{\sqrt{2}}\left(-\sqrt{\omega\tilde{D}} + i\sqrt{\omega\tilde{D}}\right). \tag{D-4}$$

Thus, the complex wave number (taking positive result) is

$$\kappa + i\alpha = \frac{\omega}{v^c} = \sqrt{\frac{\omega}{2\tilde{D}}} + i\sqrt{\frac{\omega}{2\tilde{D}}}. \tag{D-5}$$

Note that the imaginary part and real part of the complex wave number are equal. The phase velocity is given as

$$v^{\mathrm{phs}} = \kappa/\omega = \sqrt{2\omega D}. \tag{D-6}$$

With the definition of Q_V^{-1} for homogeneous waves, we have (using equation D-4)

$$Q_V^{-1} = -\mathrm{Im}(v^c)^2/\mathrm{Re}(v^c)^2 = -(-i\omega\tilde{D})/0 \to \infty. \tag{D-7}$$

With the definition of Q_T^{-1} for homogeneous waves, we have (using equations D-5 and D-6)

$$Q_T^{-1} = \frac{2\alpha v^{\mathrm{phs}}}{\omega} = \frac{2}{\omega}\sqrt{\frac{\omega}{2\tilde{D}}}\sqrt{2\omega\tilde{D}} = 2. \tag{D-8}$$

REFERENCES

Badiey, M., A. H.-D. Chen, and Y. K. Mu, 1998, From geology to geoacoustics-Evaluation of Biot-Stoll sound speed and attenuation for shallow water acoustics: Journal of the Acoustical Society of America, **103**, 309–320, doi: 10.1121/1.421136.

Berryman, J. G., and H. F. Wang, 2000, Elastic wave propagation and attenuation in a double-porosity dual-permeability medium: International Journal of Rock Mechanics and Mining Sciences, **37**, 63–78, doi: 10.1016/S1365-1609(99)00092-1.

Biot, M. A., 1956a, Theory of propagation of elastic waves in a fluid-saturated porous solid. I. Low-frequency range: Journal of the Acoustical Society of America, **28**, 168–178, doi: 10.1121/1.1908239.

Biot, M. A., 1956b, Theory of propagation of elastic waves in a fluid-saturated porous solid. II. Higher-frequency range: Journal of the Acoustical Society of America, **28**, 178–191, doi: 10.1121/1.1908241.

Biot, M. A., 1962a, Mechanics of deformation and acoustic propagation in porous media: Journal of Applied Physics, **33**, 1482–1498, doi: 10.1063/1.1728759.

Biot, M. A., 1962b, Generalized theory of acoustic propagation in porous dissipative media: Journal of the Acoustical Society of America, **34**, 1254–1264, doi: 10.1121/1.1918315.

Borcherdt, R. D., 1977, Reflection and refraction of type-II S waves in elastic an anelastic media: Bulletin of the Seismological Society of America, **67**, 43–67.

Borcherdt, R. D., 1982, Reflection and refraction of general P- and type-I S-waves in elastic and anelastic solids: Geophysical Journal of Royal Astronomical Society, **70**, 621–638, doi: 10.1111/j.1365-246X.1982.tb05976.

Borcherdt, R. D., 2009, Viscoelastic waves in layered media: Cambridge University Press.

Borcherdt, R. D., and L. Wennerberg, 1985, General P, Type-I S, and Type-II S waves in anelastic solids; Inhomogeneous wave fields in low-loss solids: Bulletin of the Seismological Society of America, **75**, 1729–1763.

Buchen, P. W., 1971, Plane waves in linear viscoelastic media: Geophysical Journal of Royal Astronomical Society, **23**, 531–542, doi: 10.1111/j.1365-246X.1971.tb01841.x.

Carcione, J. M., 2014, Wave fields in real media. Theory and numerical simulation of wave propagation in anisotropic, anelastic porous and electromagnetic media, handbook of geophysical exploration, 3rd ed.: Elsevier.
Carcione, J. M., and F. Cavallini, 1993, Energy balance and fundamental relations in anisotropic-viscoelastic media: Wave Motion, **18**, 11–20, doi: 10.1016/0165-2125(93)90057-M.
Cerveny, V., and I. Psencik, 2005, Plane waves in viscoelastic anisotropic media — I. Theory: Geophysical Journal International, **161**, 197–212, doi: 10.1111/j.1365-246X.2005.02589.x.
Cerveny, V., and I. Psencik, 2006, Energy flux in viscoelastic anisotropic media: Geophysical Journal International, **166**, 1299–1317, doi: 10.1111/j.1365-246X.2006.03057.x.
Chen, A. H.-D., 2016, Poroelasticity, theory and applications of transport in porous media: Springer.
Kelder, O., and D. M. J. Smeulders, 1997, Observation of the Biot slow wave in water-saturated Nivelsteiner sandstone: Geophysics, **62**, 1794–1796, doi: 10.1190/1.1444279.
Liu, X., S. Greenhalgh, B. Zhou, and M. Greenhalgh, 2018, Effective Biot theory and its generalization to poro-viscoelastic methods: Geophysical Journal International, **212**, 1255–1273, doi: 10.1093/gji/ggx460.
Liu, X., S. Greenhalgh, B. Zhou, and H. J. Li, 2020, Explicit Q expressions for inhomogeneous P- and SV-waves in isotropic viscoelastic media: Journal of Geophysics and Engineering, **17**, 300–312, doi: 10.1093/jge/gxz106.
Lockett, F. J., 1962, The reflection and refraction of waves at an interface between viscoelastic materials: Journal of the Mechanics and Physics of Solids, **10**, 53–64, doi: 10.1016/0022-5096(62)90028-5.
Mandelis, A., 2000, Diffusion waves and their uses: Physics Today, **53**, 29–34, doi: 10.1063/1.1310118.
Picotti, S., and J. M. Carcione, 2017, Numerical simulation of wave-induced fluid flow seismic attenuation based on the Cole-Cole model: Journal of the Acoustical Society of America, **142**, 134–145, doi: 10.1121/1.4990965.
Plona, T., 1980, Observation of a second bulk compressional wave in porous medium at ultrasonic frequencies: Applied Physics Letters, **36**, 259–261, doi: 10.1063/1.91445.
Pride, S. R., J. G. Berryman, and J. M. Harris, 2004, Seismic attenuation due to wave-induced flow: Journal of Geophysical Research, **109**, B01201, doi: 10.1029/2003JB002639.
Pride, S. R., and M. W. Haartsen, 1996, Electroseismic wave properties: Journal of the Acoustical Society of America, **100**, 1301–1315, doi: 10.1121/1.416018.
Turgut, A., and T. Yamamoto, 1988, Synthetic seismograms for marine sediments and determination of porosity and permeability: Geophysics, **53**, 1056–1067, doi: 10.1190/1.1442542.